The finding of a novel small DNA lesion with high thermal resistance and stability under basic conditions

Taishu Kawada[1,2,3], Katsuhito Kino* [1,4], Akito Komi[1], Haruna Nishiyama[2], Rina Tsuboi[2], Akane Sakaga[2], Mayu Araki[2], Masayuki Morikawa[5], Yasuko Okamoto[5], Yoshiyuki Tanaka[5], Kiyohiko Kawai[6], and Mamoru Fujitsuka[7]

[1] Department of Nano Material and Bio Engineering, Faculty of Science and Engineering, Tokushima Bunri University, 8-53 hamano-cho, Takamatsu-shi, Kagawa 760-8542, Japan

[2] Kagawa School of Pharmaceutical Sciences, Tokushima Bunri University, 8-53 hamano-cho, Takamatsu-shi, Kagawa 760-8542, Japan

[3]Graduate School of Biomedical and Health Sciences, Hiroshima University, 1-2-3 Kasumi, Minami-ku, Hiroshima-shi, Hiroshima 734-8553, Japan

[4]Center for Advance Science and Engineering, Tokushima Bunri University, 8-53 hamano-cho, Takamatsu-shi, Kagawa 760-8542, Japan

[5]Faculty of Pharmaceutical Sciences, Tokushima Bunri University,180 Nishihama-Boji, Yamashiro-cho, Tokushima 770-8514, Japan

[6]Department of Life Science and Technology, School of Life Science and Technology, Institute of Science Tokyo, 4259 Nagatsuta-cho, Midori-ku, Yokohama, Kanagawa 226-8501, Japan

[7]SANKEN (The Institute of Scientific and Industrial Research), The University of Osaka, Ibaraki, Osaka 567-0047, Japan

* Katsuhito Kino

Email: kkino@kph.bunri-u.ac.jp.

Author Contributions: K.Kino designed research; and T.K. and K.Kino performed research; T.K., K.Kino, A.K., H.N., R.T., A.S., M.A., M.M., Y.O., Y.T., K.Kawai and M.F. analyzed data; and T.K. and K.Kino wrote the paper.

Competing Interest Statement: The authors declare no competing interest.

Classification: Biological Sciences/Biochemistry

Keywords: small DNA lesion, oxamic acid, stability, DNA polymerase, base excision repair

This PDF file includes:

Main Text

Scheme 1

Figures 1 to 5

Abstract

DNA, which is a carrier of genetic information, can be damaged by various environmental factors. DNA damage causes mutations during DNA replication, whereas accurate DNA repair processes can prevent such mutations. Such DNA lesions are known to range in size from bulky to small. Compared with the kinds of bulky and moderate DNA lesions, those of small DNA lesions are fewer, because the loss of conjugated structures makes the molecules unstable. Therefore, discovering small DNA lesions are particularly challenging. Surprisingly, we identified a novel small lesion, oxamic acid (Oxm), which is produced under physiological conditions (pH 7.4, 37°C). Oxm exhibited remarkable stability at high temperatures and under basic conditions. Moreover, guanine was preferentially incorporated opposite Oxm by DNA polymerases, allowing a primer to be extended to full length across the lesion, and then Oxm showed the potential to induce G:C → C:G transversions. Despite this mutagenic potential, base excision repair enzymes cleaved DNA oligonucleotides containing Oxm; formamidopyrimidine-DNA glycosylase specifically recognized only the Oxm:C base pair. Based on these results, Oxm is unique relative to previously characterized lesions such as 8-oxoG and Oz, and then this lesion may play a role in the mechanisms underlying gene mutations.

Significance Statement

Most known DNA lesions are relatively bulky. In contrast, the kinds of small DNA lesions are fewer because they usually arise from degradation reactions. Herein, we found a novel small DNA lesion, Oxm, that is generated under physiological conditions and is highly resistant to heat and stable under basic conditions. Furthermore, since guanine is preferentially incorporated opposite Oxm by multiple DNA polymerases, the lesion may promote G:C → C:G transversions. Notably, formamidopyrimidine-DNA glycosylase can selectively recognize Oxm:C base pairs, potentially mitigating its mutagenicity. Our findings indicate that Oxm may contribute to mutations during DNA replication, offering new insights into the molecular basis of genetic mutations.

Main Text

Introduction

DNA damage can arise under various conditions (1-8) and lead to genetic mutations (4, 6, 9-11). These effects can be mitigated if organisms have effective repair mechanisms such as base excision repair (BER) and nucleotide excision repair (12-19). Impairment of these systems is associated with conditions such as cancer, neurological disorders, and age-related diseases (12-14, 20, 21). For example, mutations were detected in the *K-ras* oncogene and the *p53* tumor suppressor gene (22-24). Extensive research has been conducted on "bulky DNA lesions" that distort the DNA duplex, such as the 6-4 thymine dimer (6-4TT), cyclobutane thymine dimer, and acetylaminofluoreneguanine (Schemes 1 and S1) (25-37). Other studies have described "moderate DNA lesions" with molecular weights comparable to native DNA bases, such as 8-oxoguanine (8-oxoG), spiroiminodihydantoin, and guanidinohydantoin (Schemes 1 and S1) (38-56). When bulky and moderate DNA lesions obtained from purines adopt an anti-conformation and pair with guanine or adenine, the structure protrudes from the standard DNA structure and creates an environment in which it is difficult for DNA polymerases to slide during replication. For example, when 8-oxoG pairs with adenine, it adopts a syn-conformation, eliminating the protrusion (57, 58); however, not all bulky and moderate DNA lesions can adopt a syn-conformation. Therefore, only a limited number of bulky and moderate DNA lesions can pair with purines for DNA replication. In contrast, small DNA lesions, such as the abasic site (Ab), 2,5-diamino-4*H*-imidazol-4-one (Iz), and 2,2,4-triamino-5(2*H*)-oxazolone (Oz) (Schemes 1 and S1), contain fewer atoms compared with "bulky DNA lesions" and "moderate DNA lesions" (41, 59-73). These lesions, which are generated from purines, enable the insertion of purine bases on the opposite side. Thus, they do not distort the original DNA structure, and DNA replication proceeds smoothly. Therefore, with respect to replication, small DNA lesions can be considered prone to point mutations. Studying small DNA lesions is useful when considering the adverse effects of point mutations. Moreover, because they contain fewer atoms compared with native DNA bases, the types of DNA lesions

are limited. In addition, they are prone to rapid decomposition because of the loss of conjugation, thus rendering them unstable. For example, Ab gradually decomposes at room temperature (74). Iz is rapidly degraded to Oz (73); thus, identifying novel stable "small DNA lesions" is challenging.

We focused on Oz, which has the potential to induce G:C → C:G transversions (75-78). Among the four DNA bases, guanine is most susceptible to damage by oxidative stresses (e.g., ultraviolet radiation with riboflavin, visible light with methylene blue, hydrogen peroxide, peroxy radical, γ-radiation, and ultraviolet radiation) (11, 79-84). G:C → T:A and G:C → C:G transversions in DNA sequence analyses are highly induced by various oxidative stresses (79, 82, 84, 85). Although 8-oxoG, the most well-known oxidative guanine damage and a known marker of aging (86, 87), induces only G:C → T:A transversions (88, 89), Oz may induce G:C → C:G transversions (76-79) and has been detected in vivo (73, 90); however, Oz decomposes into guanidinoformimine (Gf) and Ab (69) (Schemes 1 and S1).

In this study, when Oz was decomposed, we report the discovery of oxamic acid (Oxm), a novel small DNA lesion with exceptional heat resistance and stability under basic conditions. We also describe its incorporation profile during DNA synthesis and its recognition by BER enzymes.

Results and Discussion

Discovery of Oxm

In this study, we reanalyzed Oz decomposition using 5′-TG-3′ (TG) as the raw material to maximize product separation at an absorbance of 254 nm. Next, we purified 5′-TOz-3′ (TOz) from TG through a modified method and subjected it to accelerated pyrolysis. As previously reported (69), 5′-TGf-3′ (TGf) and 5′-TAb-3′ (TAb) were produced (Figs. 1A, S1A, and S1B). Surprisingly, we discovered a novel DNA lesion, 5′-TOxm-3′ (TOxm), as the main product (45%) of TOz decomposition under pH 7.0 at 90°C for 4 h (Figs. 1A and S2J). The structure of TOxm (Fig. 1C) was purified using high-performance liquid chromatography (HPLC) and confirmed by mass spectrometry (MS) (Synapt G2-Si HDMS; Waters, USA). MS analysis revealed the following molecular ions: $[M–H]^-$, m/z = 508.0967 (Fig. 1B). Further fragmentation by MS/MS produced peaks at m/z = 464.1069, 436.1129, 338.0647, 195.0062, and 125.0350 (Fig. 1D). In addition, TOz decomposition at pH 7.4 and 37°C for 146 h yielded TOxm (Fig. 1E).

To investigate the effect of pH on TOxm formation, TOz was heated under various pH conditions (Figs. 1F and S2). In cacodylate buffer, the TOxm yield increased from 17% at pH 5 to 36% at pH 7. In phosphate buffer, yields were 24% (pH 6), 39% (pH 7), and 44% (pH 8). In borate buffer, yields were higher, reaching 49% at pH 9 and 47% at pH 10. Notably, the yield at pH 13 (48%; Fig. S3) was similar to that at pH 9 and pH 10. These results indicate that basic conditions promote TOxm formation and enhance its stability compared with acidic conditions. Subsequently, we examined TOxm degradation at 90°C for 2 h. At pH 13, only 2% of TOxm was decomposed (Fig. S4B), whereas at pH 3, 58% was decomposed (Fig. S4D). The addition of H^+ to the carbonyl group of Oxm renders it susceptible to nucleophilic attack by water, which is thought to promote the reaction to Ab under acidic conditions. Thus, TOxm is highly stable under basic conditions. Similar to T8-oxoG (Fig. S5), TOxm remained stable in alkaline environments.

Previous studies on DNA lesion detection have employed hot piperidine treatment (91-94). Using this method, we analyzed whether Oxm-containing DNA oligomers undergo cleavage. Only 3% cleavage occurred at 90°C and 2% at 65°C, with no detectable cleavage at 30°C or 25°C (Figs. 2A and S6). The same result was obtained when using a negative control containing 8-oxoG (Fig. 2A). Conversely, DNA oligomers containing Oz were readily cleaved by piperidine treatment, with efficiencies of 6% at 25°C, 20% at 30°C, 70% at 65°C, and 76% at 90°C (Fig. 2A). These results show that Oxm, like 8-oxoG, is resistant to piperidine cleavage unlike Oz. The guanidino group of Oz is easier to protonate compared with the carbonyl group of Oxm, and the absence of the guanidino group in Oxm likely reduces its susceptibility to nucleophilic attack by cyclic secondary amines compared with Oz (Fig. 2B and 2C).

Analysis of Oxm using DNA polymerases

Because Oxm has remarkable stability, it may be present in the cell. If Oxm does not have the same hydrogen bonding mode as guanine, DNA polymerases may cause mutations. Therefore, to determine the mutagenic effect of Oxm, we analyzed nucleotide incorporation and DNA synthesis using DNA polymerases (Figs. 3, 4, and S7).

Overall, DNA polymerases incorporate guanine opposite Oxm. For example, DNA polymerases α, δ, ε, and ζ, despite all belonging to the B family, preferentially incorporated guanine opposite Oxm (Fig. 3B–D, lanes 7–10; Fig. 4A, lanes 7–10). In addition, other DNA polymerases, except for REV1, incorporated only guanine opposite to Oxm (Fig. S7A–E, lanes 7–10). Oxm contains a COO^- group, such as Oz (76, 95, 96), that may pair with guanine. In addition, melting temperature (*Tm*) measurements indicated that the Oxm:G base pair was slightly more stable compared with other Oxm-containing base pairs (Fig. S8). Consequently, further detailed analyses are warranted.

Next, we analyzed DNA extension across Oxm using DNA polymerases. DNA polymerases α, δ, and ε extended a 15-mer primer to a full-length 30-mer across Oxm (Fig. 3B–D, lane 6). Notably, the elongation efficiency for δ and ε was markedly lower compared with α. This difference may be due to the 3′→5′ exonuclease activity of δ and ε, which can reduce both nucleotide insertion opposite DNA lesions and elongation efficiency (97-100).

During DNA replication, the presence of DNA lesions in the template can arrest replication fork progression, resulting in its collapse, double-strand break formation, and genome instability (101); however, cells have a mechanism for elongating replication forks stalled at DNA lesion sites (102). This mechanism is known as translesion synthesis. To compensate for low translesion synthesis efficiency using DNA polymerases α, δ, and ε, we analyzed DNA extension across Oxm using DNA polymerases ζ and η, which participate in translesion synthesis and lack exonuclease activity (103-106).

DNA polymerase ζ extended across Oxm (Fig. 4A, lane 6). This performance was comparable to that of the B-family polymerase α. DNA polymerase ζ plays a key role in UV mutagenesis (107-109), and its elongation efficiency varies depending on the lesion. For example, elongation across Oz proceeds with the same efficiency as that across native DNA (78), and polymerase ζ can bypass 6-4 TT (110), 8-oxoG (111), and Ab (112), although the extension efficiencies for these lesions are lower than those across native bases (110-112). Overall, elongation efficiency by polymerase ζ follows the trend: Oz > Oxm > 6-4TT > 8-oxoG > Ab. The relatively low efficiency across 8-oxoG may be due to the larger size of these lesions compared with guanine, whereas the smaller size of Oz and Oxm may allow them to fit more easily into the catalytic pocket of DNA polymerase ζ. In contrast, Ab creates a gap in the template strand, likely destabilizing the double-stranded structure and reducing extension efficiency. These observations suggest that the size of the catalytic pocket is a crucial factor influencing translesion synthesis by polymerase ζ and that Oxm and Oz fit well into its catalytic pocket.

DNA polymerase η, a member of the Y family, extended to full length beyond Oxm (Fig. 4B, lane 6). The efficiency of elongation across Oxm was comparable to that across guanine (Fig. 4B, lanes 1 and 6). These results indicate that Oxm is a substrate for elongation by DNA polymerase η. Why did DNA polymerase η show higher efficiency for elongation across Oxm than DNA polymerase ζ? DNA polymerase η can directly elongate across many DNA lesions (e.g., 6-4TT, DNA adducts, 8-oxoG, Gh, and Ab) (113-116). In contrast, DNA polymerase ζ performs elongation after other DNA polymerases have incorporated bases opposite of the DNA lesions (117, 118). Based on these findings, DNA polymerase ζ is considered to have less efficiency for elongation across any lesion compared with DNA polymerase η (106, 110, 117, 118). This may also explain our result that efficiency across Oxm is higher for DNA polymerase η compared with DNA polymerase ζ (Figs. 4A, B, lane 6).

Moreover, the elongation efficiency across Oxm was calculated relative to that across guanine, yielding the following extension efficiencies: DNA polymerase η > DNA polymerase ζ and α >> DNA polymerase δ and ε. DNA polymerases δ and ε preferentially incorporated dGTP opposite Oxm and extended past it to a limited extent, suggesting that Oxm can slightly induce G:C → C:G transversions in normal DNA replication. The addition of DNA polymerases ζ and η to the normal DNA replication system significantly increased the probability of Oxm-mediated G:C → C:G transversions.

Incision activity of formamidopyrimidine-DNA glycosylase for Oxm

The analysis of Oxm using DNA polymerases suggests that Oxm may induce G:C → C:G transversions. When repair enzymes remove Oxm from Oxm:C base pairs, which are produced from G:C, the original genetic information is maintained (Fig. 5A). In contrast, after DNA polymerases incorporate guanine opposite Oxm, BER enzymes remove Oxm from Oxm:G, thereby not restoring the original genetic information (Fig. 5A). Therefore, to accurately repair Oxm, BER enzymes must exhibit low activity for Oxm:G and high activity for Oxm:C (Fig. 5A).

Moreover, Oxm is also similarly stable to 8-oxoG with respect to piperidine treatment. Since nucleophilic attack by a cyclic secondary amine initiates BER by formamidopyrimidine-DNA glycosylase (Fpg) (119), we investigated whether Oxm, which resists piperidine nucleophilicity, is a substrate for Fpg.

DNA oligomers containing Oxm paired with G, A, or T were minimally cleaved by Fpg (Fig. 5C, lanes 16–18). In contrast, Fpg selectively cleaved the oligomer containing Oxm paired with C (Fig. 5C, lane 15). Consistent with previous reports (120), Fpg did not cleave DNA oligomers containing 8-oxoG paired with A but cleaved those with 8-oxoG paired with C, G, or T (Fig. 5C, lanes 3–6). In addition, DNA oligomers containing Oz paired with C, G, A, and T were cleaved by Fpg with similar efficiencies (Fig. 5C, lanes 9–12). If Oz is repaired before Oxm formation, base incorporation by DNA polymerases opposite Oxm would be irrelevant. However, given that Fpg selectively recognizes Oxm:C, Oxm may play a more significant detrimental role in the organism than Oz.

Previously, the base pairing of 8-oxoG has been characterized by X-ray crystallography (57, 58). For Fpg to cleave the oligomer containing 8-oxoG, it must recognize the carbonyl group (C=O) at the 8-position and the N–H group at the 7-position of 8-oxoG in the anti-conformation (121, 122). Accordingly, Fpg recognizes the anti-conformation of 8-oxoG paired with C, G, or T but not the syn-conformation paired with A. The fact that Fpg cleaves the oligomer containing Oxm paired with C suggests that the Oxm:C base pair may adopt a conformation similar to the 8-oxoG:C base pair. Moreover, Fpg cleaves Oxm:C base pairs more efficiently than 8-oxoG:C base pairs. These findings support the idea that Fpg helps prevent G:C → C:G transversions caused by Oxm and attempts to restore the original genetic information (Fig. 5A).

We also examined whether other DNA repair enzymes selectively recognize the Oxm:C base pair. Endonuclease III and endonuclease VIII do not specifically recognize Oxm:C (Fig. S9, lanes 9-12). Thus, it remains necessary to identify other repair enzymes that selectively recognize the Oxm:C base repair.

Limitations and future prospects

In this study, we discovered a novel small DNA lesion, Oxm. High Oxm stability provides a strong incentive for future studies to detect the formation of Oxm directly in vivo, similar to that of other lesions (123). In addition, urea (Ua) was produced from Oz (Figs. 1A and S1C); however, Ua generation mechanisms need to be examined in the future. Furthermore, X, the decomposition product of Oxm (Fig. S4D), appears to be an isomer of Oxm, because the mass of TX was the same as that of TOxm (Figs. 1B and S1D). To analyze X, a new method is needed to prepare it in large quantities.

Oxm does not halt DNA replication, and this DNA lesion may cause G:C → C:G transversions that are not caused by 8-oxoG. It will be important to analyze whether such mutations induced by Oxm occur in vivo and to verify whether Oxm is as valuable as 8-oxoG in elucidating the underlying mechanisms of various diseases caused by acquired mutations. Moreover, it is important to determine how translesion synthesis (i) and BER (ii) circumvent Oxm-mediated mutations.

(i) REV1 incorporates cytosine opposite of Oxm (Fig. S7F, lane 7), and it collaborates with DNA polymerase ζ (108, 109, 124-127). Whether DNA polymerase ζ elongates across Oxm after REV1 incorporates cytosine opposite this DNA lesion in vivo warrants further study.

(ii) *Escherichia coli* Fpg accurately repairs Oxm, and its activity was comparable to that of 8-oxoG. It will be necessary to find a human enzyme that can correctly repair Oxm (Fig. 5A).

Materials and Methods

Enzymes

T4 polynucleotide kinase, Fpg, endonuclease III (Nth) and endonuclease VIII (Nei) were purchased from New England Biolabs (Ipswich, USA). Taq DNA polymerase and Vent exo$^-$ were obtained from Bio Basic Inc. (Ontario, Canada). T4 DNA ligase and *Pyrobest* DNA polymerase were purchased from Takara (Otsu,

Japan). Calf thymus DNA polymerase α and human DNA polymerase β were purchased from Chimerx (Milwaukee, USA). Kf exo$^-$ was purchased from Fermentas (Waltham, USA). Yeast DNA polymerase ζ was purchased from Enzymax (Lexington, USA). Human DNA polymerase δ (78), human DNA polymerase η (79), Saccharomyces cerevisiae DNA polymerase ε (128), and hREV1$_{(341–829)}$ (78) were purified as previously described.

Oxm production

Riboflavin was purchased from Kishida Chemical Co., Ltd. (Osaka, Japan). A controller (Model CL-1501) and LED sources emitting at 450 nm (Model CL-H1-450-9-1-B; 2.75–275 mW/cm^2) were purchased from Asahi Spectra Co., Ltd. (Tokyo, Japan) for the photooxidation experiments. Triethylamine and acetonitrile were purchased from FUJIFILM Wako Pure Chemical Industries, Ltd. (Osaka, Japan). HPLC was performed using the LC-2000Plus series (pump: PU-2080; PDA detector: MD-2015; oven: CO-2060; gradient mixer: MX-2080-32) from JASCO Corporation (Tokyo, Japan). The standard phosphoramidite method was applied to synthesize the 5′-TG-3′ oligonucleotide.

The reaction solution contained 100 μM 5′-TG-3′, 75 μM riboflavin, and 10 mM cacodylate buffer (pH 7.0). This mixture was photooxidized to 5′-TIz-3′ by LED irradiation (450 nm) at 27.5 mW/cm^2 for 2 min in the presence of riboflavin, following a previously described method (129). Next, Tlz was hydrolyzed to 5′-TOz-3′ using a modified version of the previous method (73). Specifically, TIz was incubated in 5 mM cacodylate buffer (pH 7.0) at 65°C for 75 min. Subsequently, 5′-TOz-3′ was purified by HPLC using a COSMOSIL PBr packed column (Nacalai Tesque; 5 μm, 150 × 4.6 mm), with an elution gradient of 3–7% acetonitrile (CH_3CN) in 50 mM TEAA (pH 7) over 20 min at a flow rate of 1.0 mL/min. Absorbance was monitored at 254 nm. The collected fractions were desalted using Sep-Pak C18 Plus Short Cartridge (Waters, Nihon Waters K.K., Tokyo, Japan). The desalted 5′-TOz-3′ (50 μM) was incubated in 50 mM cacodylate buffer (pH 7.0) at 90°C for 4 h. The resulting mixture was analyzed by HPLC (Figs. 1A and S2J) and confirmed using MS (Figs. 1B and D) (Synapt G2-Si HDMS, Nihon Waters K.K., Tokyo, Japan).

Alternatively, when 5′-TIz-3′ was incubated at 90°C for 10 min in 10 mM NaOH/KCl buffer (pH 13), 5′-TOxm-3′ was quickly generated (Fig. S10).

Effect of pH on Oxm

Reaction mixtures containing 50 μM desalted TOz and 50 mM buffer were incubated at 90°C for 4 h. Buffers used included cacodylate buffer (pH 5, 6, 7), phosphate buffer (pH 6, 7, 8), borate buffer (pH 8, 9, 10), and NaOH/KCl buffer (pH 13). The reaction mixture was analyzed by HPLC using a COSMOSIL PBr Packed Column (Nacalai Tesque, 5 μm, 150 × 4.6 mm), elution with a solvent mixture of 50 mM TEAA (pH 7), 3–6% CH_3CN/0–20 min and 6% (isocratic)/20–30 min at a flow rate of 1.0 mL/min, and the absorbance was monitored at 254 nm.

Furthermore, reaction mixtures containing 30 μM desalted TOxm and 50 mM buffer (fresh citrate buffer, pH 3; NaOH/KCl buffer, pH 13) were incubated at 90°C for 2 h. They were analyzed by HPLC under the same conditions described above.

DNA oligomer

The DNA template (5′-CTCATCAACATCTTGAATTCACAATCAATA-3′), complementary 30-mer DNA oligomers (5′-TATTGATTGTGAATTWAAGATGTTGAT-GAG -3′, where W represents C, G, A, or T), Alexa 680-labeled 30-mer DNA oligomers (5′-Alexa 680-CTCATCAACATCTTXAATTCACAATCAATA-3′, where X represents G or 8-oxoG), Alexa 680-labeled 15-mer primer (5′-Alexa 680-TATTGATTGTGAATT-3′), 6-mer DNA oligomer (5′-CTTGAA-3′), 13-mer DNA oligomer (5′-TTCACAATCAATA-3′), 11-mer DNA oligomer (5′-CTCATCAACAT-3′), and Alexa 680-labeled 11-mer DNA oligomer (5′-Alexa 680-CTCATCAACAT-3′) were synthesized and obtained from Japan Bio Services Co., Ltd. (Saitama, Japan).

First, the 6-mer DNA oligomer (5′-CTTGAA-3′) was oxidized to generate a 6-mer oligomer containing Iz (6-mer Iz; 5′-CTTXAA-3′, where X represents Iz) using LED irradiation at 450 nm in the presence of riboflavin, following a previously described method (73,129). The 6-mer DNA oligomer containing Oz (6-

mer Oz; 5′-CTTXAA-3′, where X represents Oz) was then obtained from 6-mer Iz (78). Specifically, 6-mer Iz was incubated in 5 mM cacodylate buffer (pH 7.0) at 65°C for 75 min. Next, a 6-mer oligomer containing Oxm (6-mer Oxm; 5′-CTTXAA-3′, where X represents Oxm) was obtained by heating the 6-mer Oz at 90°C for 4 h. The 6-mer Oxm was purified using HPLC with a CHEMCOBOND 5-ODS-H column (Chemco Plus Scientific Co., Ltd., Osaka, Japan; 5 μm, 150 × 4.6 mm) with elution by 7–9% acetonitrile (CH_3CN) in 50 mM TEAA (pH 7) over 30 min at a flow rate of 1.0 mL/min and confirmed by MS (Fig. S11A). Absorbance was monitored at 260 nm. The collected fractions were desalted using a Sep-Pak C18 Plus Short Cartridge. Subsequently, the 6-mer Oxm and a 13-mer DNA oligomer (5′-TTCACAATCAATA-3′) were phosphorylated using the T4 polynucleotide kinase. A 30-mer DNA template containing Oxm (30-mer Oxm; 5′-CTCATCAACATCTTXAATTCACAATCAATA-3′, where X represents Oxm) was assembled by ligating the 11-mer DNA oligomer (5′-CTCATCAACAT-3′) to the 5′ side of the 6-mer Oxm and the phosphorylated 13-mer DNA oligomer to the 3′ side using the T4 DNA ligase. The ligation was performed using a 30-mer DNA-RNA chimeric oligonucleotide (5′-TATTGATTgTGAATTGCAGATgTTGATGAG-3′, where "g" indicates guanosine) as the template. Finally, the 30-mer Oxm was purified by HPLC under the same conditions described above and confirmed by MS (Fig. S11B). Alexa 680-labeled 30-mer DNA oligomers containing Oxm or Oz (5′-Alexa 680-CTCATCAACATCTTXAATTCACAATCAATA-3′, where X represents Oxm or Oz) were prepared using the Alexa 680-labeled 11-mer DNA oligomer.

Piperidine treatment

The reaction mixture (5 μL) containing 1 M piperidine and 100 fmol Alexa 680-labeled 30-mer DNA oligomers containing G, Oxm, 8-oxoG, or Oz was incubated for 5 min at 25°C, 30°C, 65°C, or 90°C. Aliquots (2.5 μL) were then subjected to electrophoresis on a denaturing 16% polyacrylamide gel containing 8 M urea and run at 30 W for 90 min. The fluorescence intensity of each n-mer band (I_n) was quantified using an Odyssey infrared imaging system (LI-COR; Lincoln, USA) for the 5′-Alexa 680-labeled products (Fig. S6).

DNA polymerization reaction

Polymerization reactions (5 μL) were performed using the following buffer compositions: DNA polymerase α = 40 mM Tris-HCl (pH 8.0), 5 mM $MgCl_2$, 10 mM NaCl, 45 mM KCl, 1 mM DTT, 100 μg/mL bovine serum albumin (BSA); DNA polymerase β = 50 mM Tris-HCl (pH 8.8), 10 mM $MgCl_2$, 1 mM DTT, 100 μg/mL BSA; DNA polymerase δ = 50 mM Tris-HCl (pH 7.4), 2 mM $MgCl_2$, 2 mM DTT, 100 μg/mL BSA; DNA polymerase ε = 50 mM Tris-HCl (pH 7.4), 8 mM $MgCl_2$, 2 mM DTT, 100 μg/mL BSA; DNA polymerases ζ, η, and $hREV1_{(341-829)}$ = 50 mM Tris-HCl (pH 8.0), 2 mM $MgCl_2$, 5 mM DTT, 100 μg/mL BSA; Kf exo$^-$ = 50 mM Tris-HCl (pH 8.0), 5 mM $MgCl_2$, 1 mM DTT, 100 μg/mL BSA; *Pyrobest* DNA polymerase = 1× *Pyrobest* Buffer II (Takara), 100 μg/mL BSA; *Taq* DNA polymerase = 1× Taq reaction buffer (Bio Basic Inc.), 100 μg/mL BSA; Vent exo$^-$ = 20 mM Tris-HCl (pH 8.8), 10 mM $(NH_4)_2SO_4$, 10 mM KCl, 2 mM $MgCl_2$, 1 mg/mL BSA.

The reaction mixtures for DNA polymerases α, β, δ, ε, η, ζ, Kf exo$^-$, *Pyrobest* DNA polymerase, *Taq* DNA polymerase, Vent exo$^-$, and hREV1 contained 100 fmol of the DNA template containing G or Oxm and 50 fmol of a 5′-Alexa 680-labeled 15-mer primer. Other reaction conditions and dNTP and DNA polymerase concentrations are detailed in the figure legends. Reactions were performed at 30°C for 30 min for DNA polymerases α, β, δ, ε, ζ, Kf exo$^-$, *Pyrobest* DNA polymerase, *Taq* DNA polymerase, and Vent exo$^-$; at 37°C for 30 min for DNA polymerase η; and at 30°C for 10 min for $hREV1_{(341–829)}$. All reactions were terminated by adding 5 μL of stop buffer (15 mM EDTA, 10% glycerol, and 100 μM rhodamine 6G). Aliquots (2.5 μL) were separated by electrophoresis on a denaturing 16% polyacrylamide gel containing 8 M urea at 30 W for 90 min. The fluorescence intensity of each n-mer band (I_n) was quantified using an Odyssey infrared imaging system (LI-COR; Lincoln, USA).

Measurement of Tm for Oxm

DNA oligomers containing Cy3 (5′-TATTGATZTGTGAATTYAAGATGTTGATGAG-3′, where Y represents C, G, A, or T, and Z represents Cy3) were synthesized by Gene Design Inc. (Osaka, Japan). The 30-mer oligomer containing C (30-mer C: 5′-CTCATCAACATCTTXAATTCACAATCAATA-3′, where X represents C) was synthesized by Japan Bio Services Co., Ltd. (Saitama, Japan). The 30-mer oligomer containing Oxm (30-mer Oxm: 5′-CTCATCAACATCTTXAATTCACAATCAATA-3′, where X represents Oxm) was prepared as described in the main text. The fluorescence of the DNA sample (strand concentration: 4 nM Cy3-labeled oligomers, 8 nM 30-mer C or 30-mer Oxm, 100 mM NaCl, 10 mM $MgCl_2$, 7.5% PEG-20,000, 10 mM Na phosphate buffer [pH 7.0]) was monitored at 572 nm (I_{572}; excitation at 533 nm) from 37°C to 87°C with a heating rate of 1°C/min using a Roche LightCycler 96 real-time PCR system. *T*m values were determined as the peak of the $\Delta I_{572}/\Delta T$ plot versus the temperature (130).

Repair enzyme reaction

Reaction mixtures (5 μL) were prepared as follows: Fpg = 1× NEBuffer 1 (New England Biolabs), 0.1 mg/mL BSA, 50 fmol Alexa 680-labeled 30-mer DNA oligomers containing G, Oxm, 8-oxoG, or Oz, 100 fmol complementary 30-mer DNA oligomers, and 4 mU Fpg; Nei = 1× Endonuclease VIII Reaction buffer (New England Biolabs), 0.1 mg/mL BSA, 50 fmol Alexa 680-labeled 30-mer DNA oligomers containing Oxm or Oz, 100 fmol complementary 30-mer DNA oligomers, 71 mU Nei; Nth = 1× endonuclease III reaction buffer (New England Biolabs), 0.1 mg/mL BSA, 50 fmol Alexa 680-labeled 30-mer DNA oligomers containing Oxm or Oz, 100 fmol complementary 30-mer DNA oligomers, and 500 mU Nth. The reaction mixtures were incubated at 30°C for 60 min. All reactions were terminated by adding 5 μL of stop buffer (15 mM EDTA, 10% glycerol, and 100 μM rhodamine 6G). Aliquots (2.5 μL) were analyzed by electrophoresis on a denaturing 16% polyacrylamide gel containing 8 M urea at 30 W for 90 min. The fluorescence intensity of each n-mer band was quantified using an Odyssey infrared imaging system (LI-COR; Lincoln, USA) for 5′-Alexa 680-labeled products.

Acknowledgments

Special thanks to Mr. Hitoki Mitani from Tokushima Bunri University. This work was supported by JSPS KAKENHI 17K00558 and 23K11427. In addition, K. Kino's idea in this manuscript was gotten on the basis of my other studies supported by research grants from LNest Grant LRAD Award, from Radiation Effects Association, from the Nakatomi Foundation and from the Japan Prize Foundation, and then I am grateful for the foundations. The authors would like to thank Enago (www.enago.jp) for the English language review.

References

1. A.-M. Fleminga, J.-C. Dingmana, C.-J. Burrows, CO_2 protects cells from iron-Fenton oxidative DNA damage in *Escherichia coli* and humans. *Proc. Natl. Acad. Sci. U.S.A.* 121, e2419175121 (2024).
2. D. Aerssens, E. Cadoni, L. Tack, A. Madder, A photosensitized singlet oxygen ($^1O_2$) toolbox for bio-organic applications: Tailoring $^1O_2$ generation for DNA and protein labelling, targeting and biosensing. *Molecules* 27, 778 (2022).
3. K. Hirakawa, S. Okazaki, H. Murakami, N. Kanayama, Development of cancer-selective and effective photosensitizers through electron transfer mechanism. *J. Jpn. Soc. Laser Surg. Med*. 41, 349–355 (2021).
4. E. Dumont, A. Monari, Understanding DNA under oxidative stress and sensitization: The role of molecular modeling. *Front. Chem*. 3, 43 (2015).
5. B.-H. Yun, P.-C. Dedon, N.-E. Geacintov, V. Shafirovich, One-electron oxidation of a pyrenyl photosensitizer covalently attached to DNA and competition between its further oxidation and DNA hole injection. *Photochem. Photobiol*. 86, 563–570 (2010).
6. S. Kawanishi, Y. Hiraku, S. Oikawa, Mechanism of guanine-specific DNA damage by oxidative stress and its role in carcinogenesis and aging *Mutat. Res*. 488, 65–76 (2001).

7. K. Kino *et al.*, The oxidation of 8-oxo-7,8-dihydroguanine by iodine. *Bioorg. Med. Chem. Lett*. 20, 3818–3820 (2010).
8. S. Steenken, S.-V. Jovanovic, How easily oxidizable is DNA? One-electron reduction potentials of adenosine and guanosine radicals in aqueous solution. *J. Am. Chem. Soc*. 119, 617–618 (1997).
9. N. Liu, J. Du, J. Ge, S.-B. Liu, DNA damage-inducing endogenous and exogenous factors and research progress. *Nucleosides Nucleotides Nucleic Acids* 14, 1-33 (2024).
10. N. Kumar, S. Raja, B.-V. Houten, The involvement of nucleotide excision repair proteins in the removal of oxidative DNA damage. *Nucleic Acids Res*. 48, 11227-11243 (2020).
11. N.J. Sargentini, K.C. Smith, DNA sequence analysis of γ-radiation (anionic)-induced and spontaneous lacI^{d} mutations in *Escherichia coli* K-12. *Mutat. Res*. 309, 147–163 (1994).
12. C.-E. Halim, S. Deng, K.-C. Crasta, C.-T. Yap, Interplay between the cytoskeleton and DNA damage response in cancer progression. *Cancers* 17, 1378 (2025).
13. H.-E. Krokan, M. Bjøras, Base excision repair. *Cold Spring Harb. Perspect. Biol*. 5, a012583 (2013).
14. S. Zhao, S.-L. Habib, A.-G. Senejani, M. Sebastian, D. Kidane, Role of base excision repair in innate immune cells and its relevance for cancer therapy. *Biomedicines* 10, 557 (2022).
15. M. Kolbanovskiy, A. Aharonoff, A.-H. Sales, N.-E Geacintov, V. Shafirovich, Base and nucleotide excision repair pathways in DNA plasmids harboring oxidatively generated guanine lesions. *Chem. Res. Toxicol*. 34, 1, 154–160 (2021).
16. J. A. Marteijn, H. Lans, W. Vermeulen, J. H. Hoeijmakers, Understanding nucleotide excision repair and its roles in cancer and ageing. *Nat. Rev. Mol. Cell Biol*. 15, 465−481 (2014)
17. O,-D. Schärer, Nucleotide excision repair in eukaryotes. *Cold Spring Harb Perspect Biol*. 5, a012609, (2013).
18. P.-J. Berti, J.-A.-B. McCann, Toward a detailed understanding of base excision repair enzymes: Transition state and mechanistic analyses of N-Glycoside Hydrolysis and N-Glycoside Transfer. *Chem. Rev*. 106, 506−555 (2006).
19. E.C. Friedberg *et al.*, DNA Repair and Mutagenesis, 2nd Edition, *ASM Press*, Washington, DC, (2005).
20. W. Zhou *et al.*, Base excision repair in human cancer: Emerging diagnostic and therapeutic target. *DNA Repair* 152, 103879 (2025).
21. J.-A. Brinkman, Y. Liu, S.-J. Kron, Small-molecule drug repurposing to target DNA damage repair and response pathways. *Semin. Cancer Biol*. 68, 230–241 (2021).
22. H.-M. Khaled *et al.*, Correlation between p53 mutations and HPV in bilharzial bladder cancer. *Urol. Oncol*. 21, 334−341 (2003).
23. F. Maehira *et al.*, Alterations of protein kinase C, 8-hydroxydeoxyguanosine, and K-ras oncogene in rat lungs exposed to passive smoking. *Clin. Chim. Acta.* 289, 133−144 (1999).
24. W. Giaretti *et al.*, Specific K-ras2 mutations in human sporadic colorectal adenomas are associated with DNA near-diploid aneuploidy and inhibition of proliferation. *Am. J. Pathol*. 153, 1201−1209 (1998).
25. O. Adebalia, A. Sancarc, C.-P. Selby, Dynamics of transcription- coupled repair of cyclobutane pyrimidine dimers and (6-4) photoproducts in *Escherichia coli*. *Proc. Natl. Acad. Sci. U.S.A.* 121, e2416877121 (2024).
26. A.-H. Sales *et al.*, Inhibition of *E. coli* RecQ helicase activity by structurally distinct DNA lesions: Structure—Function relationships. *Int. J. Mol. Sci. 23*, 15654 (2022).
27. L. Sarmini, N. Kitsera, M. Meabed, A. Khobta, Transcription blocking properties and transcription-coupled repair of N^2-alkylguanine adducts as a model for aldehyde-induced DNA damage. *J. Biol. Chem*. 301, 108459 (2025).
28. M.-K. Tang *et al.*, Reactions of [^{13}C]-labelled tobacco smoke with DNA to generate selected adducts formed without metabolic activation. *Carcinogenesis*, 46, bgaf008 (2025).
29. Y. Chen, R.-E. Johnson, R.-A. Manderville, J. Liu, A high-affinity and selective DNA aptamer for the *N*-linked C8-deoxyguanosine adduct produced by the arylamine carcinogen 4-aminobiphenyl. *Chem. Res. Toxicol*. 38, 340−346 (2025).

30. M. Dylewska *et al.*, AlkA glycosylase and AlkB dioxygenase constitute an effective protective system for endogenously arising acrolein. *J. Mol. Biol*. 437, 168912 (2025).
31. C.-K. Au, S. Nagl, W. Chan, Effects of heavy metal Co-exposure on the formation of DNA adducts from aristolochic acid I: Implications for balkan endemic nephropathy development. *Chem. Res. Toxicol*. 37, 545−548 (2024).
32. Y.-E.-R. Jeong, R.-W. Kung, J.-Bykowski, T.-K. Deak, S.-D. Wetmore, Effect of guanine adduct size, shape, and linker type on the conformation of adducted DNA: A DFT and molecular dynamics study. *J. Phys. Chem*. B 127, 9035−9049 (2023).
33. M. Bellamri *et al.*, Nuclear DNA and mitochondrial damage of the cooked meat carcinogen 2-amino-1-methyl-6-phenylimidazo[4,5-*b*]pyridine in human neuroblastoma cells. *Chem. Res. Toxicol.* 36, 1361−1373 (2023).
34. Y. Fu *et al.*, Base-displaced intercalated structure of the 3-(2-deoxy-β-D-erythropentofuranosyl)-pyrimido[1,2-*f*]purine-6,10(3*H*,5*H*)-dione (6-oxo-M_1dG) lesion in DNA. *Chem. Res. Toxicol*. 36, 1947−1960 (2023).
35. K.-Y. Wu *et al.*, Dose-response formation of N7-(3-benzo[1,3]dioxol-5-yl-2-hydroxypropyl) guanine in liver and urine correlates with micronucleated reticulocyte frequencies in mice administered safrole oxide. *Food Chem. Toxicol.* 181, 114056 (2023).
36. P.-L. Li *et al.*, An unprecedented free radical mechanism for the formation of DNA adducts by the carcinogenic N-sulfonated metabolite of aristolochic acids. *Free Radic Biol. Med*. 205, 332-345 (2023).
37. S.-S. Bagale *et al.*, Synthesis of N^2-*trans*-isosafrole-dG-adduct bearing DNAs and the bypass studies with human TLS polymerases *κ* and *η*. *J. Org. Chem*. 89, 7680−7691 (2024).
38. N.-A. Johnson, R. McKenzie, L. McLean, L.-C Sowers, H.-M Fletcher, 8-oxo-7,8-dihydroguanine is removed by a nucleotide excision repair-like mechanism in *Porphyromonas gingivalis* W83. *J. Bacteriol*. 186, 7697-7703 (2004).
39. S. Jang *et al.*, UV-DDB stimulates the activity of SMUG1 during base excision repair of 5-hydroxymethyl-2'-deoxyuridine moieties. *Nucleic Acids Res*. 51, 4881-4898 (2023).
40. T. Sugiyama, M.-R. Sanyal, Biochemical analysis of H_2O_2-induced mutation spectra revealed that multiple damages were involved in the mutational process. *DNA Repair* 134, 103617 (2024).
41. A.-D. Stolyarenko, A.-A. Novikova, E.-S. Shilkin, V.-A. Poltorachenko, A.-V. Makarova, The catalytic activity of human REV1 on undamaged and damaged DNA. *Int. J. Mol. Sci*. 25, 4107 (2024).
42. A. Galli *et al.*, Ligation-mediated polymerase chain reaction detection of 8-oxo-7,8-dihydro-2′-deoxyguanosine and 5-hydroxycytosine at the codon 176 of the p53 gene of hepatitis C-associated hepatocellular carcinoma patients. *Int. J. Mol. Sci*. 21, 6753 (2020).
43. M. Kolbanovskiy, A. Aharonoff, A.-H. Sales, N.-E. Geacintov, V. Shafirovich, Recognition and repair of oxidatively generated DNA lesions in plasmid DNA by a facilitated diffusion mechanism. *Biochem. J*. 478, 2359–2370 (2021).
44. P.-L. McKibbin *et al.*, Repair of hydantoin lesions and their amine adducts in DNA by base and nucleotide excision repair. *J. Am. Chem. Soc*. 135, 13851−13861 (2013).
45. V. Shafirovich, K. Kropachev, M. Kolbanovskiy, N.-E. Geacintov, Excision of oxidatively generated guanine lesions by competing base and nucleotide excision repair mechanisms in human cells. *Chem. Res. Toxicol*. 32, 753−761 (2019).
46. A.-H. Sales *et al.*, Treatment of human HeLa cells with black raspberry extracts enhances the removal of DNA lesions by the nucleotide excision repair mechanism. *Antioxidants*, 11, 2110 (2022).
47. E.-R. Lotsof *et al.*, NEIL1 recoding due to RNA editing impacts lesion-specific recognition and excision. *J. Am. Chem. Soc*. 144, 14578−14589 (2022).
48. M.-D. Leipold, J.-G. Muller, C.-J. Burrows, S.-S. David, Removal of hydantoin products of 8-oxoguanine oxidation by the Escherichia coli. *Biochemistry* 39, 14984-14992 (2000).
49. V. Duarte, J.-G. Muller, C.-J. Burrows, Insertion of dGMP and dAMP during in vitro DNA synthesis opposite an oxidized form of 7,8-dihydro-8-oxoguanine. *Nucleic Acids Res*. 27, 496-502 (1999).

50. H.-W. Servius, A.-C. Drohat, Characterizing the excision of 7,8-dihydro-8-oxoadenine by thymine DNA glycosylase. *J. Biol. Chem*. 301, 110363 (2025)
51. A.-L. Rozelle, Y. Cheun, C.-K. Vilas, M.-C. Koag, S. Lee, DNA interstrand cross-links induced by the major oxidative adenine lesion 7,8-dihydro-8-oxoadenine. *Nat. Commun*. 12, 1897 (2021).
52. J.-J. Mäkinen, P. Rosenqvist, P. Virta, M. Metsä-Ketelä, G.-A. Belogurov, Probing the nucleobase selectivity of RNA polymerases with dual-coding substrates. *J. Biol. Chem*. 300, 107755 (2024).
53. H. Jung, S. Lee, Promutagenic bypass of 7,8-dihydro-8-oxoadenine by translesion synthesis DNA polymerase Dpo4. *Biochem. J*. 477, 2859-2871 (2020).
54. M. Wojciechowski, H. Czapinska, J. Krwawicz, D. Rafalski, M. Bochtler, Cytosine analogues as DNA methyltransferase substrates. *Nucleic Acids Res*. 52, 9267-9281 (2024).
55. Y. Sakurai *et al.*, Synthesis and properties of nucleobase-sugar dual modified nucleic acids: 2′-OMe-RNA and scpBNA bearing a 5-hydroxycytosine nucleobase. *J. Org. Chem*. 88, 154−162 (2023).
56. T. Yokogawa *et al.*, dUTPase inhibition confers susceptibility to a thymidylate synthase inhibitor in DNA-repair-defective human cancer cells. *Cancer Sci*. 112, 422-432 (2021).
57. L.-A. Lipscomb *et al.*, X-ray structure of a DNA decamer containing 7,8-dihydro-8-oxoguanine. *Proc. Natl. Acad. Sci. U.S.A*. 92, 719-723 (1995).
58. V.-K. Batra, D.-D. Shock, W.-A. Beard, C.-E. McKenna, S.-H. Wilson, Binary complex crystal structure of DNA polymerase β reveals multiple conformations of the templating 8-oxoguanine lesion. *Proc. Natl. Acad. Sci. U.S.A*. 109, 113-118 (2012).
59. C. Bryan, J. Cepeda, B. Li, K. Yang, DNA−protein cross-links derived from abasic DNA lesions: Recent progress and future directions. *Chem. Res. Toxicol.* 38, 997−1005 (2025).
60. C. Bryan, K. Yang, Human 8-Oxoguanine glycosylase OGG1 cleaves abasic sites and covalently conjugates to 3'-DNA termini via cysteine and histidine addition. *ChemBioChem 26*, e202400705 (2025).
61. R. Tomar, S. Li, M. Egli, M.-P. Stone, Replication bypass of the *N*-(2-deoxy-D-*erythro*-pentofuranosyl)-urea DNA lesion by human DNA polymerase η. *Biochemistry*, 63, 754−766 (2024).
62. R. Tomar *et al.*, Base excision repair of the *N*-(2-deoxy-D-*erythro*-pentofuranosyl)-urea lesion by the hNEIL1 glycosylase. *Nucleic Acids Res*. 51, 3754-3769 (2023).
63. T. Kawada *et al.*, Analysis of nucleotide insertion opposite urea and translesion synthesis across urea by DNA polymerases. *Genes Environ*. 44, 7 (2022).
64. B.-T. Karwowski, The influence of clustered DNA damage containing Iz/Oz and ^{OXO}dG on the charge transfer through the double helix: A theoretical study. *Molecules*, 29, 2754 (2024).
65. T. Suzuki, M. Takeuchi, A. Ozawa-Tamura, Reactions of 3′,5′-di-O-acetyl-2′-deoxyguansoine and 3′,5′-di-O-acetyl-2′-deoxyadenosine to UV light in the presence of uric acid. *Genes Environ*. 44, 4 (2022).
66. B.-Z. Zhu, M. Tang, C.-H. Huang, L. Mao, J. Shao, Mechanistic study on oxidative DNA damage and modifications by haloquinoid carcinogenic intermediates and disinfection byproducts. *Chem. Res. Toxicol*. 34, 1701−1712 (2021).
67. D. Hernández-Álvarez *et al.*, Aging, physical exercise, telomeres, and sarcopenia: A narrative review. *Biomedicines*, 11, 598 (2023).
68. C.-M.-C. Andrés, J.-M.-P.-l. Lastra, C.-A. Juan, F.-J. Plou, E. Pérez-Lebeña, Chemical insights into oxidative and nitrative modifications of DNA. *Int. J. Mol. Sci*. 24, 15240 (2023).
69. D. Stathis, U. Lischke, S.-C. Koch, C.-A. Deiml, T. Carell, Discovery and mutagenicity of a guanidinoformimine lesion as a new intermediate of the oxidative deoxyguanosine degradation pathway. *J. Am. Chem. Soc*. 134, 4925−4930 (2012).
70. Y. Sato *et al.*, Synthetic DNA binders for fluorescent sensing of thymine glycol-containing DNA duplexes and inhibition of endonuclease activity. *Chem. Commun*. 59, 6088 (2023).
71. S. Delaney, J.-C. Delaney, J.-M. Essigmann, Chemical-biological fingerprinting: Probing the properties of DNA lesions formed by peroxynitrite. *Chem. Res. Toxicol.* 20, 1718-1729 (2007).

72. V. Duarte, D. Gasparutto, M. Jaquinod, J. Cadet, In vitro DNA synthesis opposite oxazolone and repair of this DNA damage using modified oligonucleotides. *Nucleic Acids Res*. 28, 1555-1563 (2000).
73. J. Cadet *et al.*, 2,2-Diamino-4-[(3,5-di-*O*-acetyl-2-deoxy-β-D-*erythro*-pentofuranosyl)amino]-5-(2*H*)-oxazolone: a novel and predominant radical oxidation product of 3′,5′-di-*O*-acetyl-2′-deoxygua-nosine. *J. Am. Chem. Soc*. 116, 7403-7404 (1994).
74. I.-G. Shishkina, F. Johnson, A new method for the postsynthetic generation of abasic sites in oligomeric DNA. *Chem. Res. Toxicol.* 13, 907–912 (2000).
75. K. Kino *et al.*, Eukaryotic DNA polymerases α, β and ε incorporate guanine opposite 2,2,4-triamino-5(2H)-oxazolone. *ChemBioChem* 10, 2613-2616 (2009).
76. M. Suzuki *et al.*, Contiguous 2,2,4-triamino-5(2*H*)-oxazolone obstructs DNA synthesis by DNA polymerases α, β, η, ι, κ, REV1 and Klenow fragment exo$^-$, but not by DNA polymerase ζ. *J. Biochem*. 159, 323-329 (2016).
77. M. Suzuki *et al.*, Analysis of nucleotide insertion opposite 2,2,4-triamino-5(2*H*)-oxazolone by eukaryotic B- and Y-family DNA polymerases. *Chem. Res. Toxicol.* 28, 1307-1316 (2015).
78. M. Suzuki *et al.*, Effects of stability of base pairs containing an oxazolone on DNA elongation. *J. Nucleic Acids* 178350 (2014).
79. K. Takimoto *et al.*, Delayed transfection of DNA after riboflavin mediated photosensitization increases G:C to C:G transversions of *supF* gene in *Escherichia coli mutY* strain. *Mutat. Res*. 445, 93–98 (1999).
80. I. Schulz, H.-C. Mahler, S. Boiteux, B. Epe, Oxidative DNA base damage induced by singlet oxygen and photosensitization: recognition by repair endonucleases and mutagenicity. *Mutat. Res*. 461, 145–156 (2000).
81. T.-J. Macbride, B.-D. Preston, L.-A. Loeb, Mutagenic spectrum resulting from DNA damage by oxygen radicals. *Biochemistry* 30, 207–213 (1991).
82. S. Akasaka, K. Takimoto, Hydrogen peroxide induces G:C to T:A and G:C to C:G transversions in the *supF* gene of *Es-cherichia coli*. *Mol. Gen. Genet*. 243, 500–505 (1994).
83. M.-R. Valentine, H. Rodriguez, J. Termini, Mutagenesis by peroxy radical is dominated by transversions at deoxyguanosine: Evidence for the lack of involvement of 8-oxo-dG and/or abasic site formation. *Biochemistry* 37, 7030–7038 (1998).
84. C.-Y. Shin, O.-N. Ponomareva, L. Connolly, M.-S. Turker, A mouse kidney cell line with a G:C→C:G transversion mutator phenotype. *Mutat. Res*. 503, 69–76 (2002).
85. K. Tano, Y. Iwamatsu, S. Yasuhira, H. Utsumi, K. Takimoto, Increased base change mutations at G:C pairs in Escherichia coli deficient in endonuclease III and VIII. *J. Radiat. Res*. 42, 409-413 (2001).
86. P. Rebecca *et al.*, Fluorescence detection of 8-oxoguanine in nuclear and mitochondrial DNA of cultured cells using a recombinant Fab and confocal scanning laser microscopy. *Free Radic Biol. Med*. 28, 987-998 (2000).
87. T. Finkel, N.-J. Holbrook, Oxidants, oxidative stress and the biology of ageing. *Nature* 408, 239–247 (2000).
88. K. Kuroda *et al.*, Possible contribution of 8-hydroxydeoxyguanosine to gene mutations in the kidney DNA of *gpt* delta rats following potassium bromate treatment. *Mutat. Res. Genet. Toxicol. Environ. Mutagen*. 894, 503729 (2024).
89. S. Shibutani, M. Takeshita, A. P. Grollman, Insertion of specific bases during DNA synthesis past the oxidation-damaged base 8-oxodG. *Nature* 349, 431−434 (1991).
90. B. Matter, D. Malejka-Giganti, A.-S. Csallany, N. Tretyakova, Quantitative analysis of the oxidative DNA lesion, 2,2-diamino-4-(2-deoxy-β-D-erythro-pentofuranosyl)amino]-5(2H)-oxazolone (oxazolone), in vitro and in vivo by isotope dilution-capillary HPLC-ESI-MS/MS. *Nucleic Acids Res*. 34, 5449-5460 (2006).
91. A.-M. Fleming, O. Alshykhly, J. Zhu, J.-G. Muller, C.-J. Burrows. Rates of chemical cleavage of DNA and RNA oligomers containing guanine oxidation products. *Chem. Res. Toxicol*. 28, 1292-1300 (2015).

92. M.-E. Johansen, J.-G. Muller, X. Xu, C.-J. Burrows, Oxidatively induced DNA-protein cross-linking between single-stranded binding protein and oligodeoxynucleotides containing 8-oxo-7,8-dihydro-2′-deoxyguanosine. *Biochemistry* 44, 5660-5671 (2005).
93. K. Nakatani, J. Shirai, S. Sando, I. Saito, Guanine specific DNA cleavage by photoirradiation of dibenzoyldiazomethane−oligonucleotide conjugates. *J. Am. Chem. Soc*. 119, 7626–7635 (1997).
94. A.-M. Maxam, W. Gilbert, Sequencing end-labeled DNA with base-specific chemical cleavaes. *Methods Enzymol*. 65, 499-560 (1980).
95. M. Suzuki *et al.*, Calculation of the stabilization energies of oxidatively damaged guanine base pairs with guanine *Molecules* 17, 6705-6715 (2012).
96. N.-R. Jena, P.-C. Mishra, Normal and reverse base pairing of Iz and Oz lesions in DNA: structural implications for mutagenesis. *RSC Adv*. 6, 64019 (2016).
97. A. Morrison, H. Araki, A.-B. Clark, R.-K. Hamatake, A. Sugino, A third essential DNA polymerase in S. cerevisiae. *Cell,* 62, 1143–1151 (1990).
98. M. Simon, L. Giot, G. Faye, DNA polymerase delta subunit of *Saccharomyces cerevisiae* is required for accurate replication. *EMBO J.* 10, 2165-2170 (1991).
99. A.-L. Morrison, A.-L. Johnson, L.-H. Johnston, A. Sugino, Pathway correcting DNA replication errors in *Saccharomyces cerevisiae*. *EMBO J.* 12, 1467-1473 (1993).
100. A. Morrison, A. Sugino, The 3′ → 5′ exonucleases of both DNA polymerases δ and ε participate in correcting errors of DNA replication in *Saccharomyces cerevisiae*. *Mol. Gen. Genet.* 242, 289-296 (1994).
101. A.-A.-L. Ler, M.-P. Carty, DNA damage tolerance pathways in human cells: A potential therapeutic target. *Front. Oncol*. 11, 822500 (2022).
102. C.-M. Kondratick, M.-T. Washington, M. Spies, Making choices: DNA replication fork recovery mechanisms. *Semin. Cell Dev. Biol*. 113, 27-37 (2021)
103. F. Yuan *et al.*, Specificity of DNA lesion bypass by the yeast DNA polymerase η. *J. Biol. Chem.* 275, 8233-8239 (2000).
104. T. Matsuda, K. Bebenek, C. Masutani, F. Hanaoka, T.-A. Kunkel, Low fidelity DNA synthesis by human DNA polymerase η. *Nature* 404, 1011-1013 (2000).
105. C. Li *et al.*, A sophisticated mechanism governs Pol ζ activity in response to replication stress. *Nat. Commun*. 15, 7562 (2024).
106. J.-R Nelson, C.-W Lawrence, D.-C Hinkle, Thymine-thymine dimer bypass by yeast DNA polymerase zeta. *Science*., 272, 1646-1649 (1996).
107. F. Zhu, M. Zhang, DNA polymerase ζ: new insight into eukaryotic mutagenesis and mammalian embryonic development. *World J. Gastroenterol*. 9, 1165-1169 (2003).
108. C.-W. Lawrence, Cellular roles of DNA polymerase ζ and Rev1 protein. *DNA Repair (Amst)* 1, 425-435 (2002).
109. C.-W. Lawrence, Cellular functions of DNA polymerase ζ and Rev1 protein. *Adv. Protein Chem*. 69, 167-203 (2004).
110. D. Guo, X. Wu, D. K.-Rajpal, J.-S. Taylor, Z. Wang, Translesion synthesis by yeast DNA polymerase ζ from templates containing lesions of ultraviolet radiation and acetylaminofluorene. *Nucleic Acids Res.* 29, 2875-2883 (2001).
111. L. Haracska, S. Prakash, L. Prakash, Yeast DNA polymerase ζ is an efficient extender of primer ends opposite from 7,8-dihydro-8-oxoguanine and O^6-methylguanine. *Mol. Cell. Biol.* 23, 1453-1459 (2003).
112. J.-R. Nelson, C.-W. Lawrence, D.-C. Hinkle, Deoxycytidyl transferase activity of yeast *REV1* protein. *Nature* 382, 729-731 (1996).
113. C. Masutani, R. Kusumoto, S. Iwai, F. Hanaoka, Mechanisms of accurate translesion synthesis by human DNA polymerase η. *EMBO J*. 19, 3100-3109 (2000).
114. A. Vaisman, C. Masutani, F. Hanaoka, S.-G. Chaney, Efficient translesion replication past oxaliplatin and cisplatin GpG adducts by human DNA polymerase η. *Biochemistry* 39, 4575-4580 (2000).

115. L. Haracska, S.-L. Yu, R.-E. Johnson, L. Prakash, S. Prakash, Efficient and accurate replication in the presence of 7,8-dihydro-8-oxoguanine by DNA polymerase η. *Nat. Genet*. 25, 458-461 (2000).
116. L. Haracska, S. Prakash, L. Prakash, Translesion synthesis by human DNA polymerase η across oxidative products of guanine. *Nucleic Acids Symp. Ser.* 48 171-172 (2004).
117. X. Zhong *et al.*, The fidelity of DNA synthesis by yeast DNA polymerase zeta alone and with accessory proteins. *Nucleic Acids Res*. 34, 4731–4742 (2001).
118. P. Garg, C.-M. Stith, J. Majka, P.-M. Burgers, Proliferating cell nuclear antigen promotes translesion synthesis by DNA polymerase zeta. *J. Biol. Chem*. 280, 23446–23450 (2005).
119. A. Katafuchi *et al.*, Differential specificity of human and *Escherichia coli* Endonuclease III and VIII homologues for oxidative base lesions. *J. Biol. Chem.* 279, 14464-14471 (2004).
120. J. Tchou *et al.*, 8-oxoguanine (8-hydroxyguanine) DNA glycosylase and its substrate specificity. *Proc. Natl. Acad. Sci. U.S.A.* 88, 4690-4694 (1991).
121. J.-C. Fromme, G.-L. Verdine, DNA lesion recognition by the bacterial repair enzyme MutM. *J. Bio. Chem*. 278, 51543-51548 (2003).
122. S.-D. Bruner, D.-P.-G. Norman, G.-L. Verdine, Structural basis for recognition and repair of the endogenous mutagen 8-oxoguanine in DNA. *Nature* 403, 859–866 (2000).
123. H. Kang *et al.*, Advances in DNA damage detection: Current progress, challenges, and future directions. *Trends Analyt. Chem*. 189, 118246 (2025).
124. S. Sharma, C.-M. Helchowski, C.-E. Canman, Differential roles for DNA polymerases eta, zeta, and REV1 in lesion bypass of intrastrand versus interstrand DNA cross-links. *Mutat. Res.* 743–744, 97–110 (2013).
125. E.-S. Shilkin *et al.*, Methylation and hydroxymethylation of cytosine alter activity and fidelity of translesion DNA polymerases. *DNA Repair* 141, 103712 (2024).
126. K. Chan, M.-A. Resnick, D.-A. Gordenin, The choice of nucleotide inserted opposite abasic sites formed within chromosomal DNA reveals the polymerase activities participating in translesion DNA synthesis. *DNA Repair* 12, 878-889 (2013).
127. J. Piao, Y. Masuda, K. Kamiya, Specific amino acid residues are involved in substrate discrimination and template binding of human REV1 protein. *Biochem. Biophys. Res. Commun*. 392, 140−144 (2010).
128. R.-K. Hamatake *et al.*, Purification and characterization of DNA polymerase II from the yeast Saccharomyces cerevisiae. Identification of the catalytic core and a possible holoenzyme form of the enzyme. *J. Biol. Chem*. 265, 4072-83 (1990).
129. T. Kawada, M. Maehara, K. Kino, Increased yields of the guanine oxidative damage product imidazolone following exposure to LED light. *Reactions* 4, 801-810 (2023).
130. K. Kawai, A. Maruyama, Triple helix conformation-specific blinking of Cy3 in DNA. *Chem. Commun*. 51, 4861 (2015).

Figures

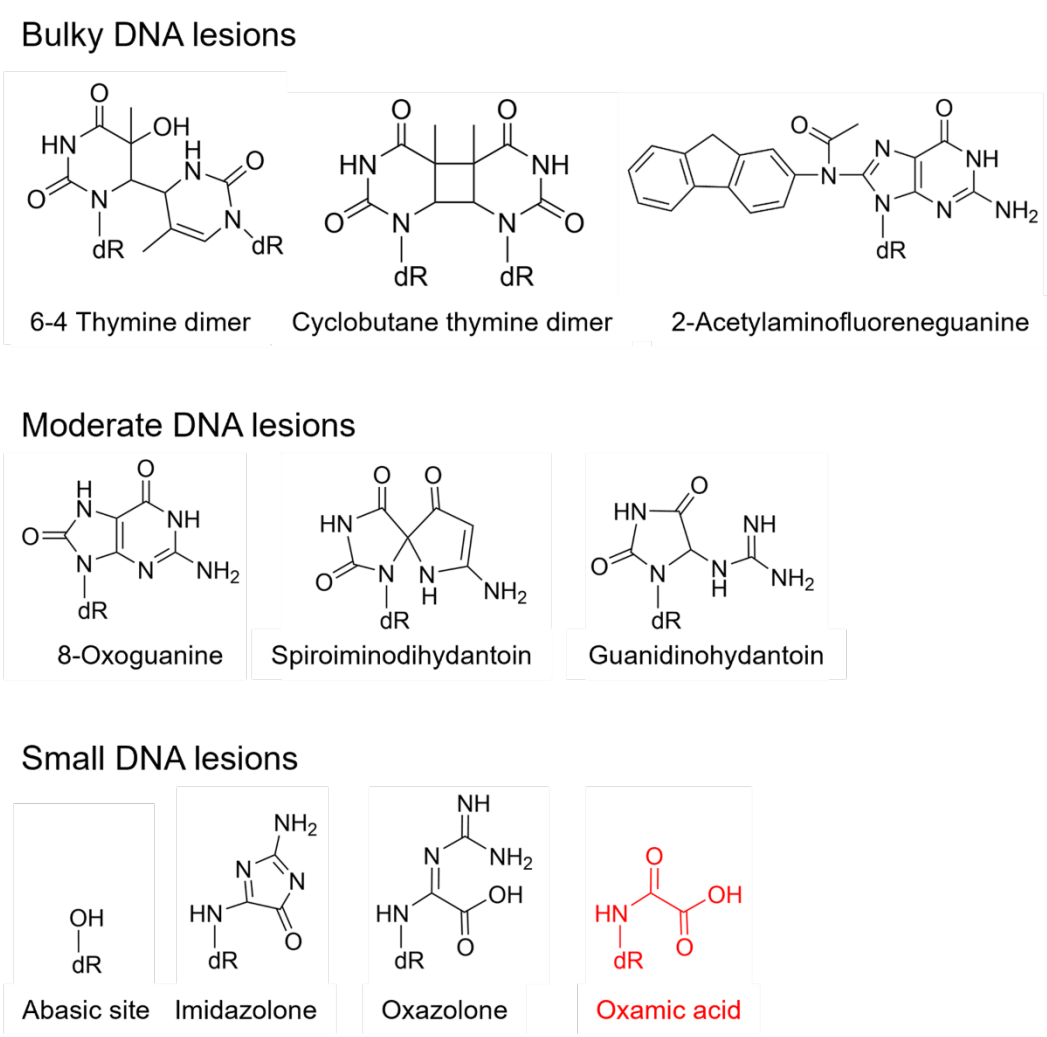

Scheme 1. Previously discovered DNA lesions (black) and the newly discovered DNA lesion (red). Other known DNA lesions are shown in Scheme S1.

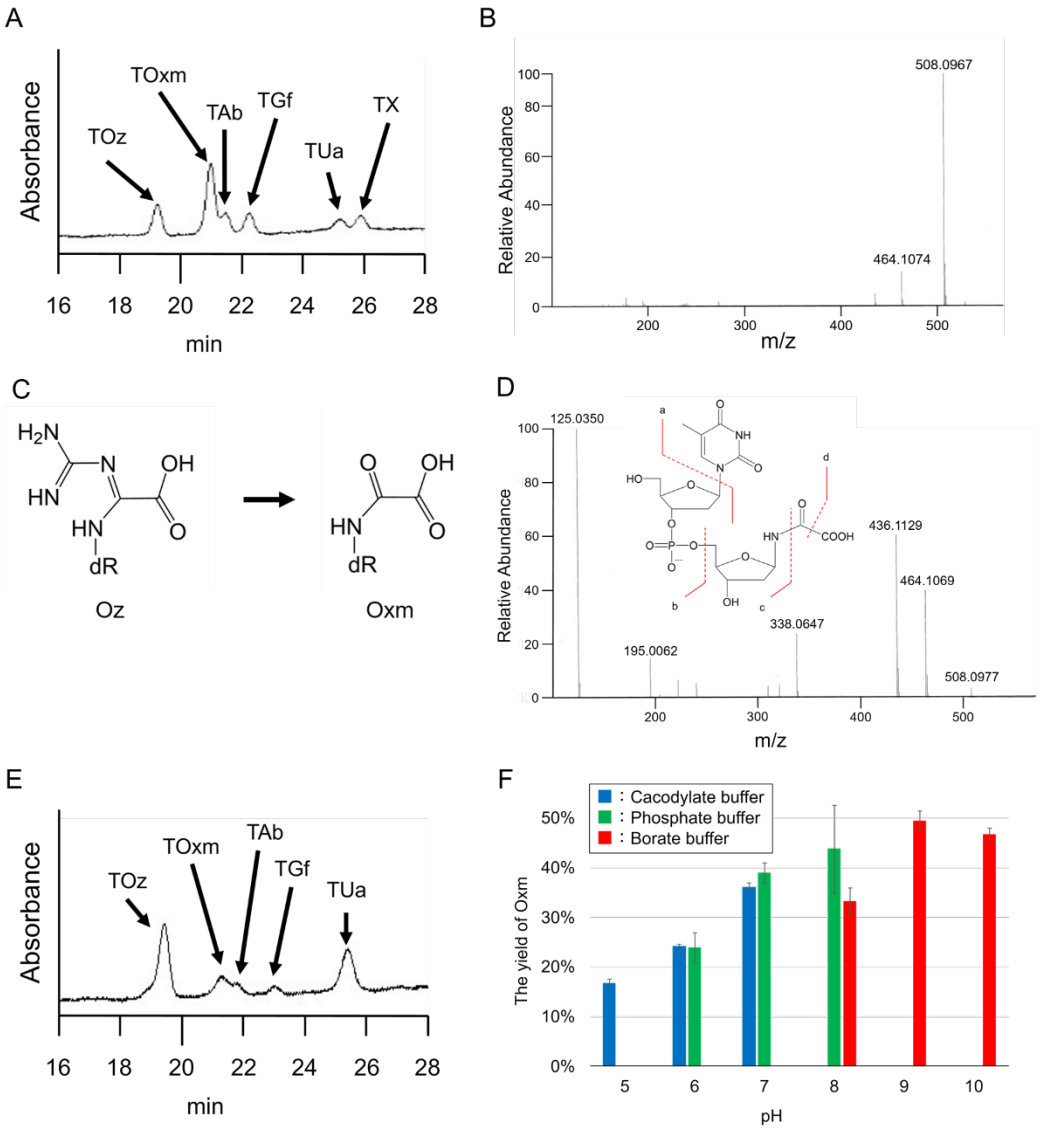

Figure 1. Discovery of Oxm. (A) HPLC analysis of DNA catabolites from 5′-TOz-3′ (TOz). Each peak (5′-TAb-3′; TAb, 5′-TUa-3′; TUa, 5′-TGf-3′; TGf) was identified by mass spectrometry (Fig S1). Raw data for (A) are shown in Fig. S2J. (B) Mass spectra of the main product (21.2 min: TOxm) from the HPLC chromatogram in (A). (C) Predicted structure of the main product derived from Oz. (D) MS/MS spectrum of TOxm. (E) Generation of Oxm at pH 7.4 and 37°C over 146 h. (F) The yield of TOxm under various pH conditions (blue: 50 mM cacodylate buffer; green: 50 mM phosphate buffer; red: 50 mM borate buffer). Bars represent mean production of Oxm for n = 2 individually prepared samples with error bars representing SD.

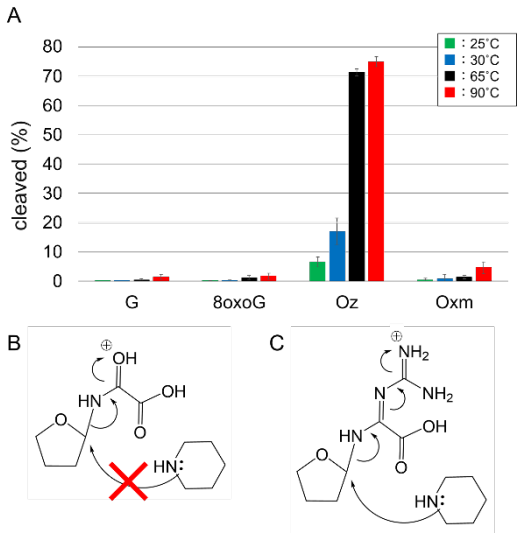

Figure 2. Piperidine treatment for Oxm. (A) Cleavage efficiency of DNA oligomers containing G, 8-oxoG, Oz, and Oxm following treatment with aqueous 1 M piperidine. The oligomers were incubated at 25°C, 30°C, 65°C, and 90°C for 5 min. Bars represent the mean cleavage efficiency of DNA oligomers for n = 3 individually prepared samples, with error bars representing SD. The raw data for (A) are shown in Fig. S6. (B, C) Proposed differences in the nucleophilic attack mechanisms on Oxm (B) and Oz (C).

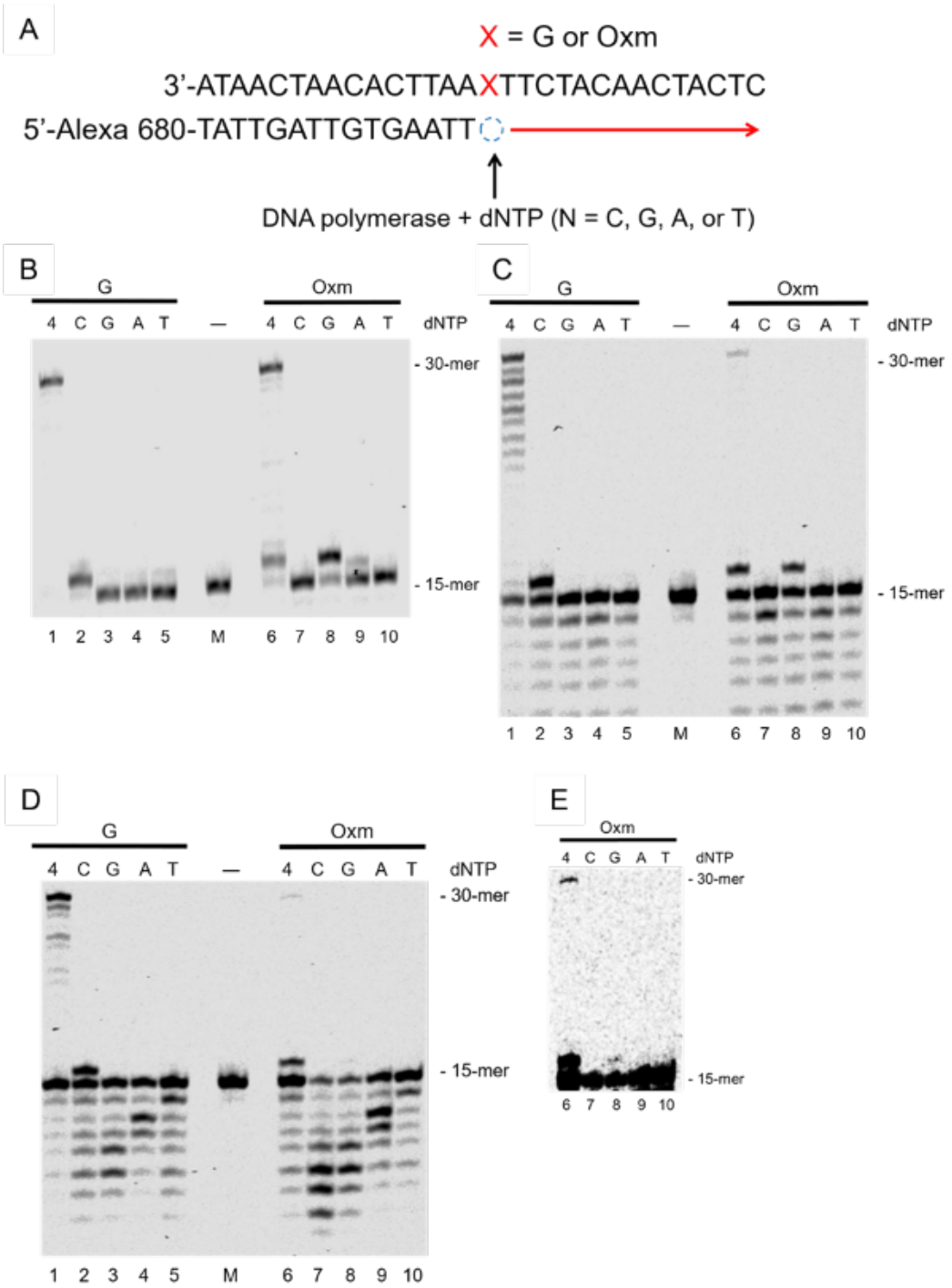

Figure 3. DNA synthesis across Oxm and nucleotide incorporation opposite Oxm. (A) Nucleotide sequences of the primers and templates. (B–E) DNA polymerase α (100 μU) (B), DNA polymerase δ (154 ng) (C), and DNA polymerase ε (50 μU) (D) were incubated with templates containing either G (lanes 1–5) or Oxm (lanes 6–10), along with 100 μM of all four dNTPs (lanes 1 and 6) or 100 μM of a single dNTP (N = C, G, A, or T) (lanes 2–5 and 7–10). Lane M contained no enzyme as a negative control. The background darkness of Panel D has been adjusted in Panel E.

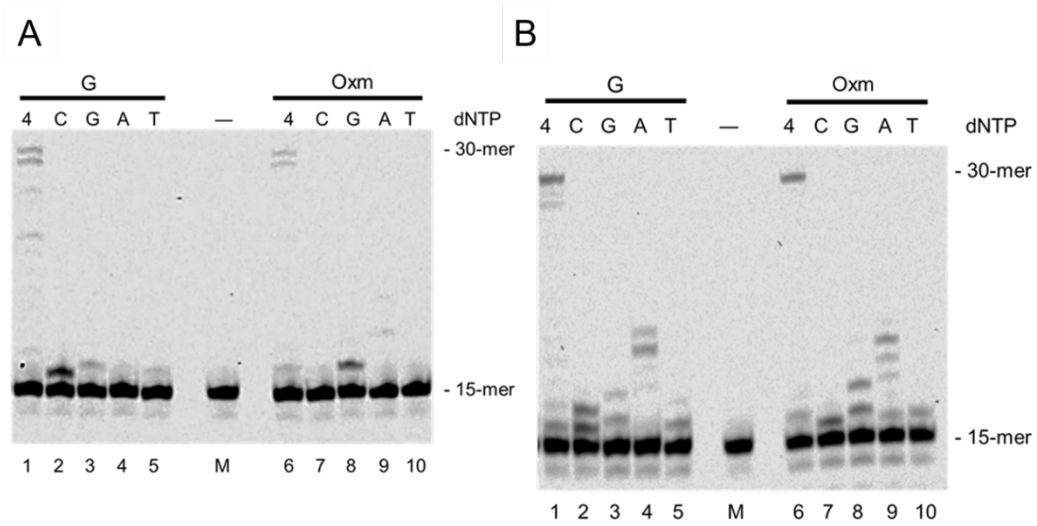

Figure 4. DNA synthesis and selective nucleotide incorporation opposite Oxm by DNA polymerase ζ (A) or DNA polymerase η (B). DNA polymerases ζ (1.7 ng) and η (0.4 ng) were incubated with templates containing either G (lanes 1–5) or Oxm (lanes 6–10), along with 100 μM of all four dNTPs (lanes 1 and 6) or 100 μM of a single dNTP (N = C, G, A, or T) (lanes 2–5 and 7–10). Lane M contained no enzyme and served as a negative control.

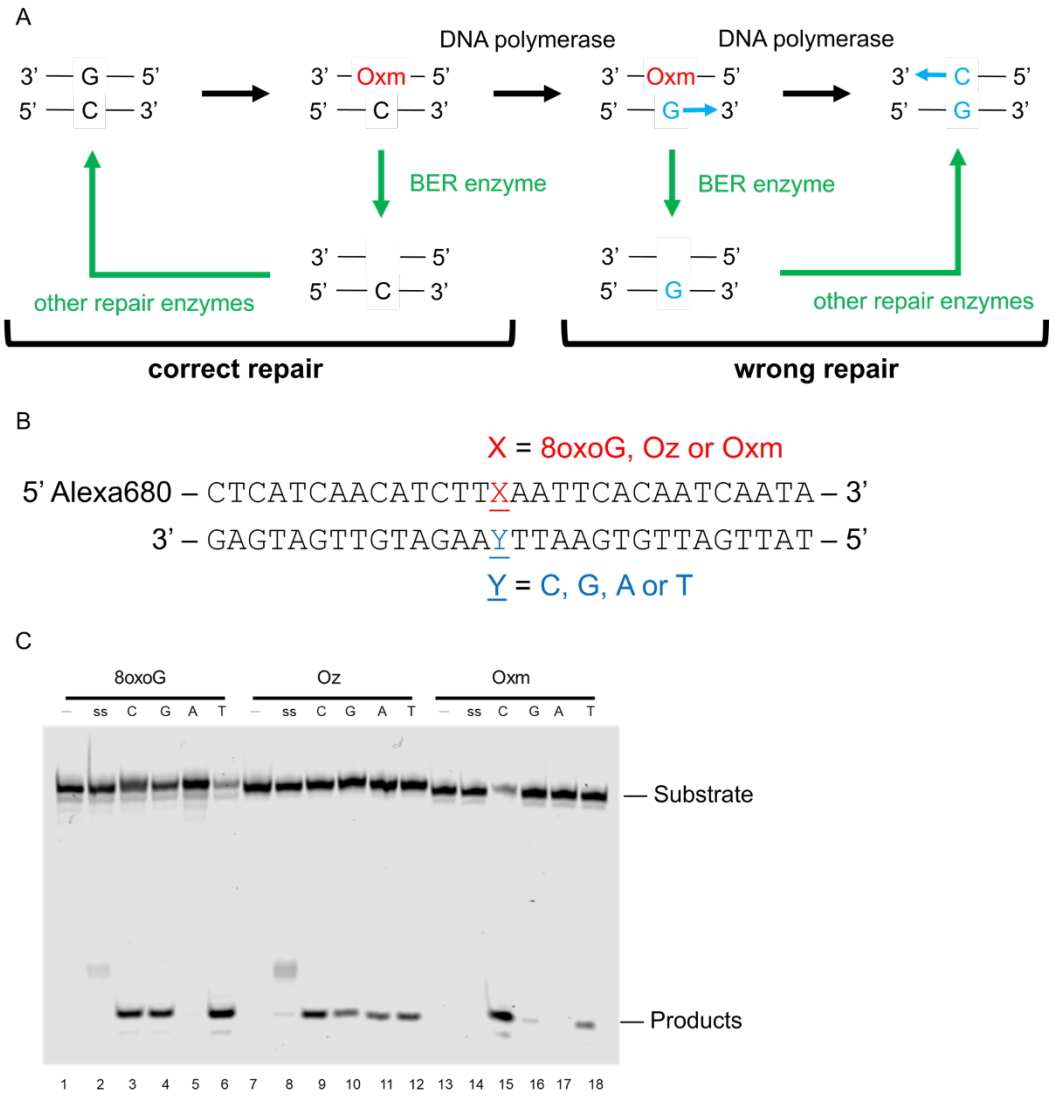

Figure 5. Incision activities of formamidopyrimidine-DNA glycosylase (Fpg). (A) Point mutation of Oxm and the repair mechanism by BER enzymes. (B) Sequences of the DNA oligomer substrates used in the experiments. (C) Fpg (4 mU) was incubated with templates containing C, G, A, or T (lanes 3–6, 9–12, and 15–18) and Alexa 680-labeled DNA oligomers containing 8-oxoG (lanes 1–6), Oz (lanes 7–12), or Oxm (lanes 13–18). Lanes 1, 7, and 13 contained no enzymes and served as negative controls. Lanes 2, 8, and 14 contained Fpg with Alexa 680-labeled DNA oligomers containing 8-oxoG, Oz, or Oxm, respectively.

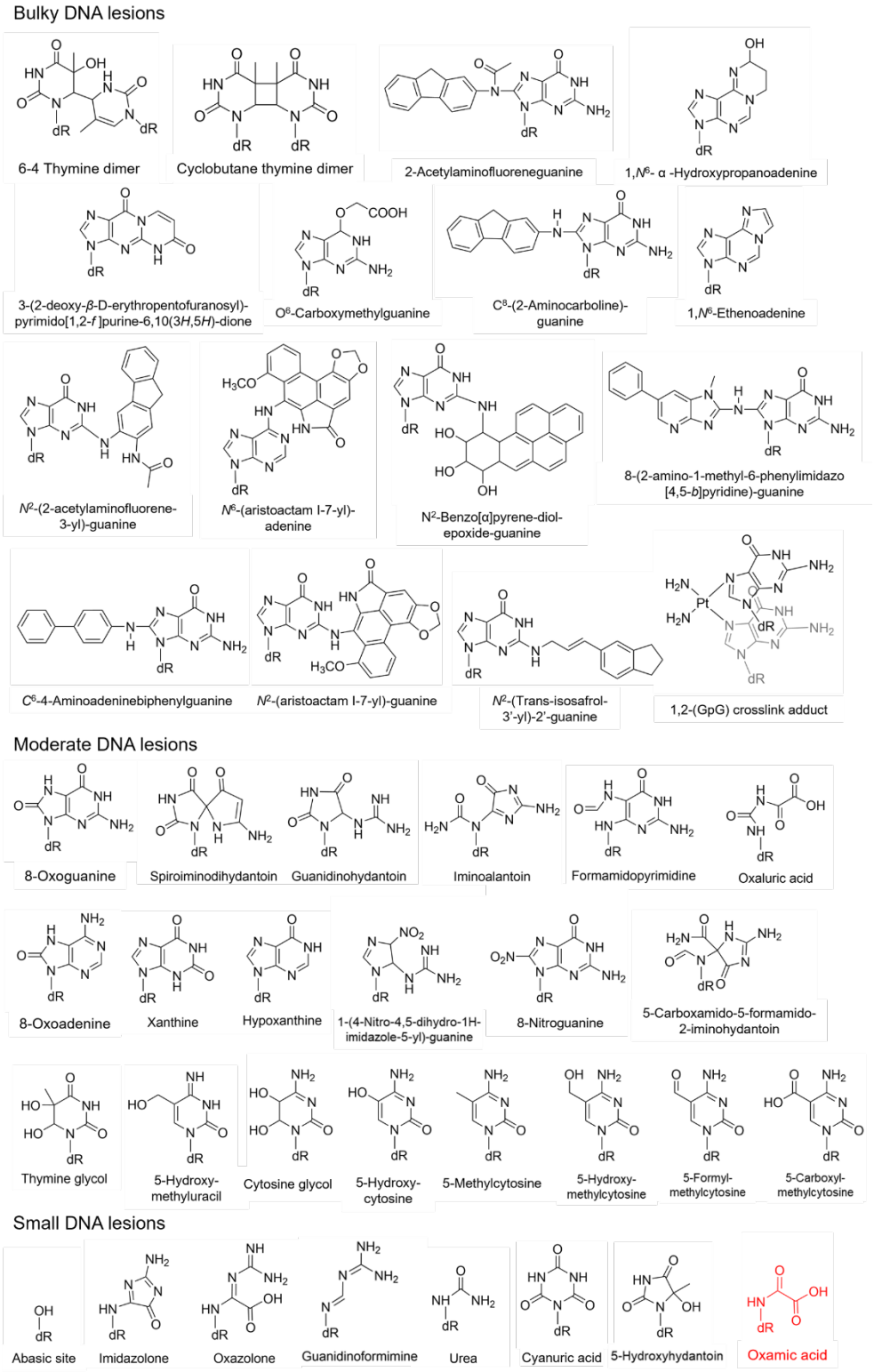

Scheme S1. Previously discovered DNA lesions (black) and the newly discovered DNA lesion (red).

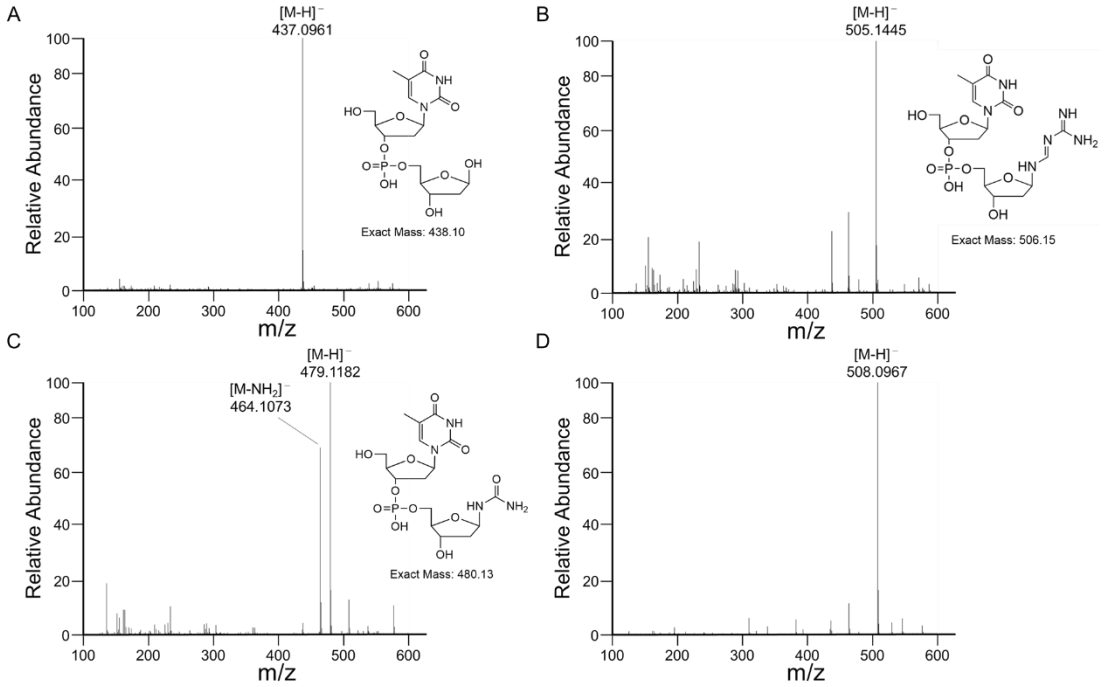

Figure S1. Mass spectra of 5′-TAb-3′ (A), 5′-TGf-3′ (B), 5′-TUa-3′ (C), and 5′-TX-3′ (D).

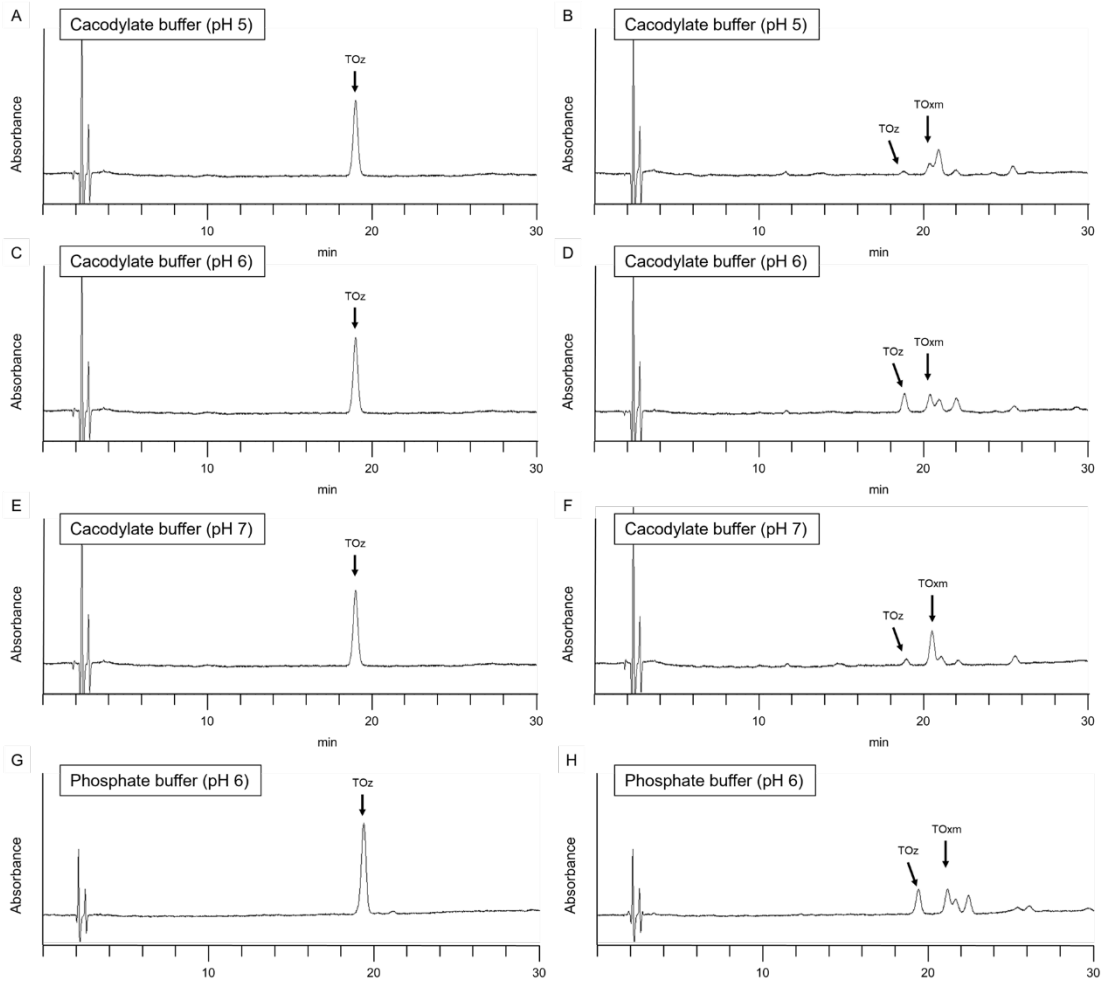

Figure S2. Generation of TOxm under various pH conditions. (A, C, E, G, I, K, M, O, Q) HPLC results of reaction mixtures for 0 h in each buffer. (B, D, F) Reaction mixtures containing TOz in cacodylate buffer (pH 5, 6, or 7) incubated at 90°C for 4 h. (H, J, L) Reaction mixtures containing TOz in phosphate buffer (pH 6, 7, or 8) incubated at 90°C for 4 h. (N, P, R) Reaction mixtures containing TOz in borate buffer (pH 8, 9, or 10) incubated at 90°C for 4 h. Yields of various peaks were calculated by setting the quantity of TOz before decomposition to 100%. All reaction mixtures were analyzed by HPLC using a COSMOSIL PBr packed column (Nacalai Tesque; 5 μm, 150 × 4.6 mm), eluted with 50 mM TEAA (pH 7) and 3–7% CH_3CN over 20–30 min at a flow rate of 1.0 mL/min. Absorbance was monitored at 254 nm.

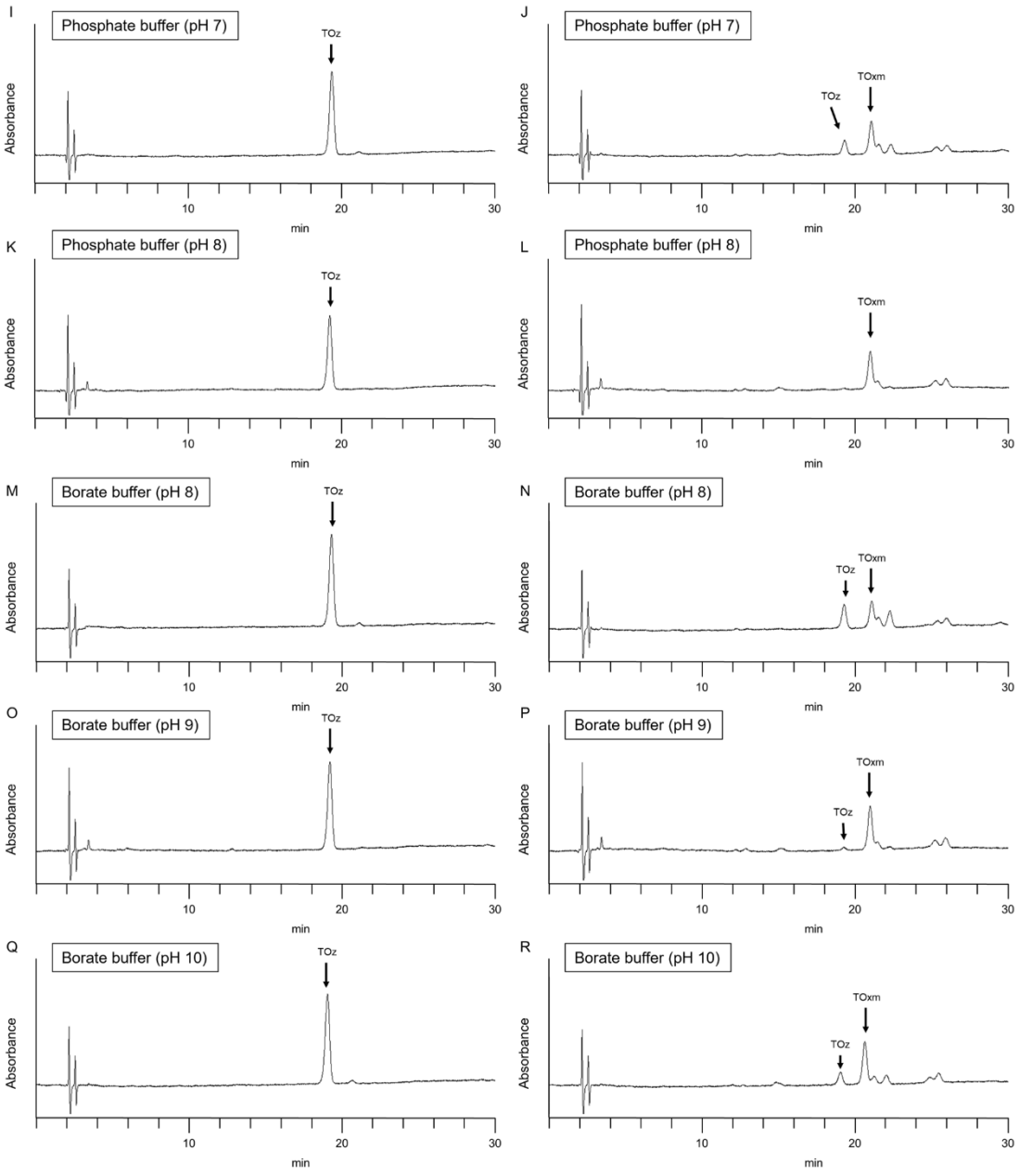

Figure S2. (*continued*)

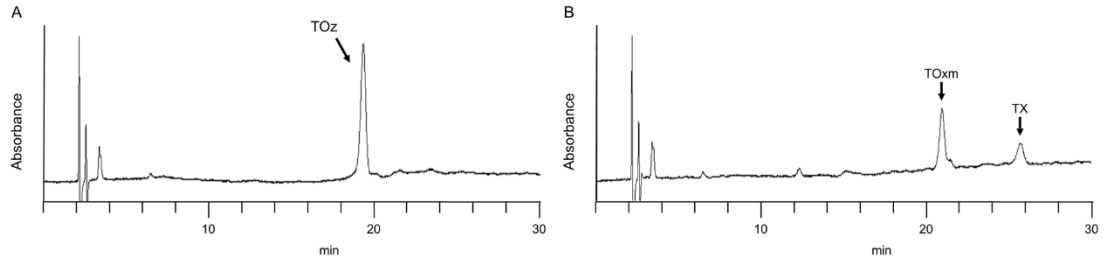

Figure S3. Pyrolysis of TOz at pH 13 and 90°C for 0 h (A) and for 4 h (B). Reaction mixtures were analyzed by HPLC using a COSMOSIL PBr packed column (Nacalai Tesque; 5 μm, 150 × 4.6 mm), eluted with 50 mM TEAA (pH 7), 3–6% CH_3CN over 20–30 min at a flow rate of 1.0 mL/min. Absorbance was monitored at 254 nm.

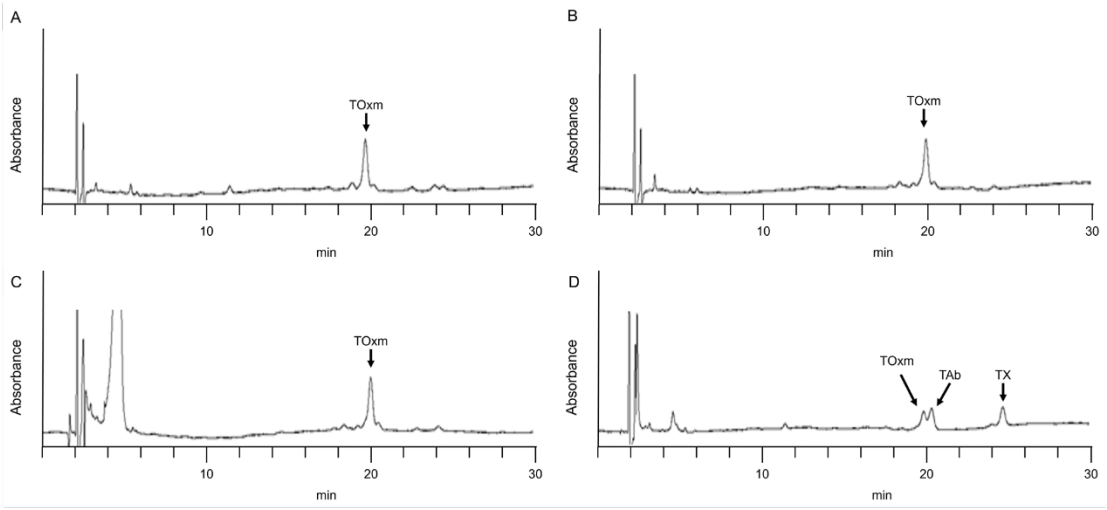

Figure S4. Stability of TOxm at 90°C under pH 13 and pH 3 conditions. (A) HPLC analysis of TOxm at pH 13 for 0 h. (B) HPLC analysis of TOxm at pH 13 for 2 h. (C) HPLC analysis of TOxm at pH 3 for 0 h. (D) HPLC analysis of TOxm at pH 3 for 2 h. Reaction mixtures were analyzed by HPLC using a COSMOSIL $5C_{18}$-MS-II packed column (Nacalai Tesque; 5 μm, 150 × 4.6 mm), eluted with 50 mM TEAA (pH 7) and 3–7% CH_3CN over 20 min at a flow rate of 1.0 mL/min. Absorbance was monitored at 254 nm.

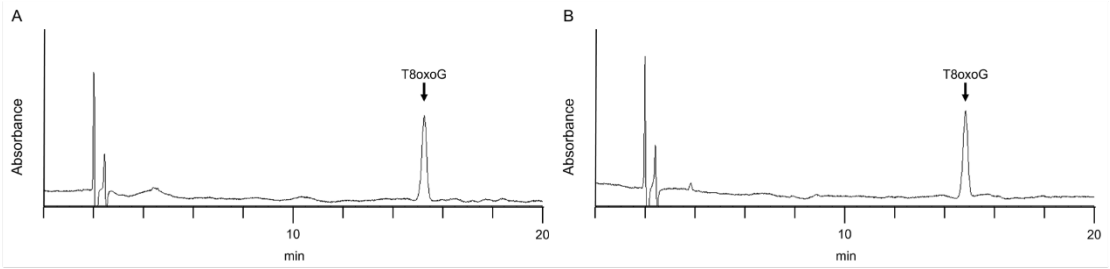

Figure S5. Stability of T8-oxoG at 90°C under basic conditions (pH 13). (A) HPLC analysis of T8-oxoG for 0 h. (B) HPLC analysis of T8-oxoG for 2 h. The reaction mixtures were analyzed by HPLC using a COSMOSIL $5C_{18}$-MS-II packed column (Nacalai Tesque; 5 μm, 150 × 4.6 mm), eluted with 50 mM TEAA (pH 7) and 3–7% CH_3CN over 20 min at a flow rate of 1.0 mL/min. The absorbance was monitored at 254 nm.

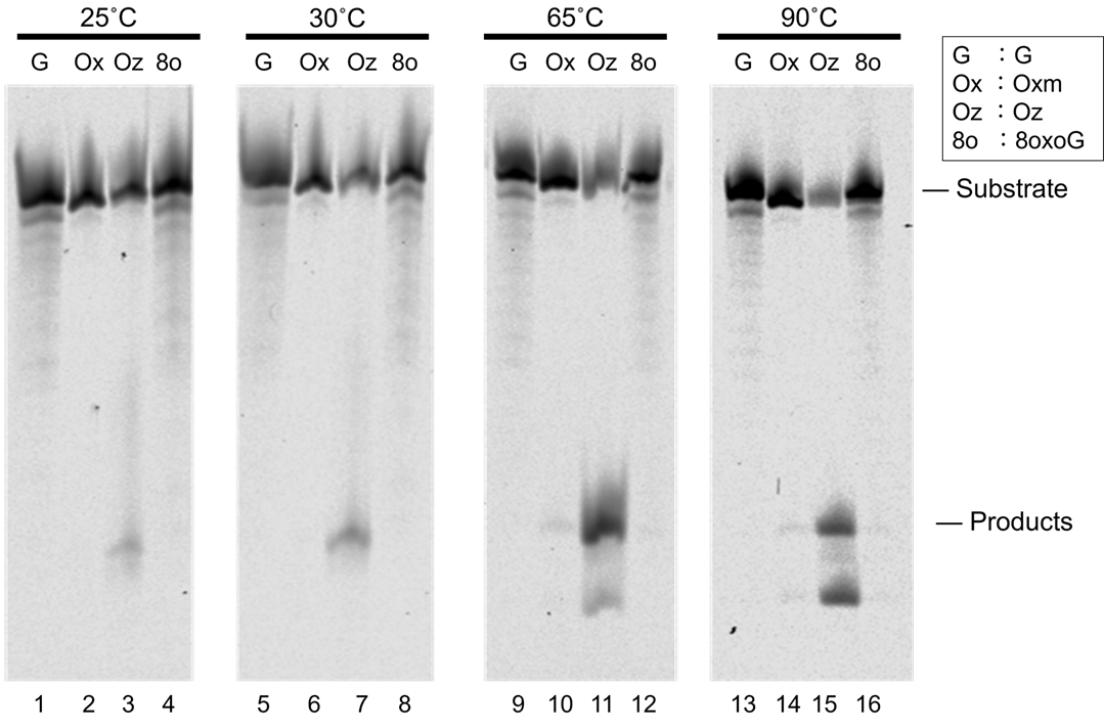

Figure S6. Piperidine treatment. The reaction mixture was incubated for 5 min at 25°C, 30°C, 65°C, or 90°C with 1 M piperidine. Each lane contains Alexa 680-labeled DNA oligomers containing G (lanes 1, 5, 9, and 13), Oxm (lanes 2, 6, 10, and 14), Oz (lanes 3, 7, 11, and 15), and 8-oxoG (lanes 4, 8, 12, and 16).

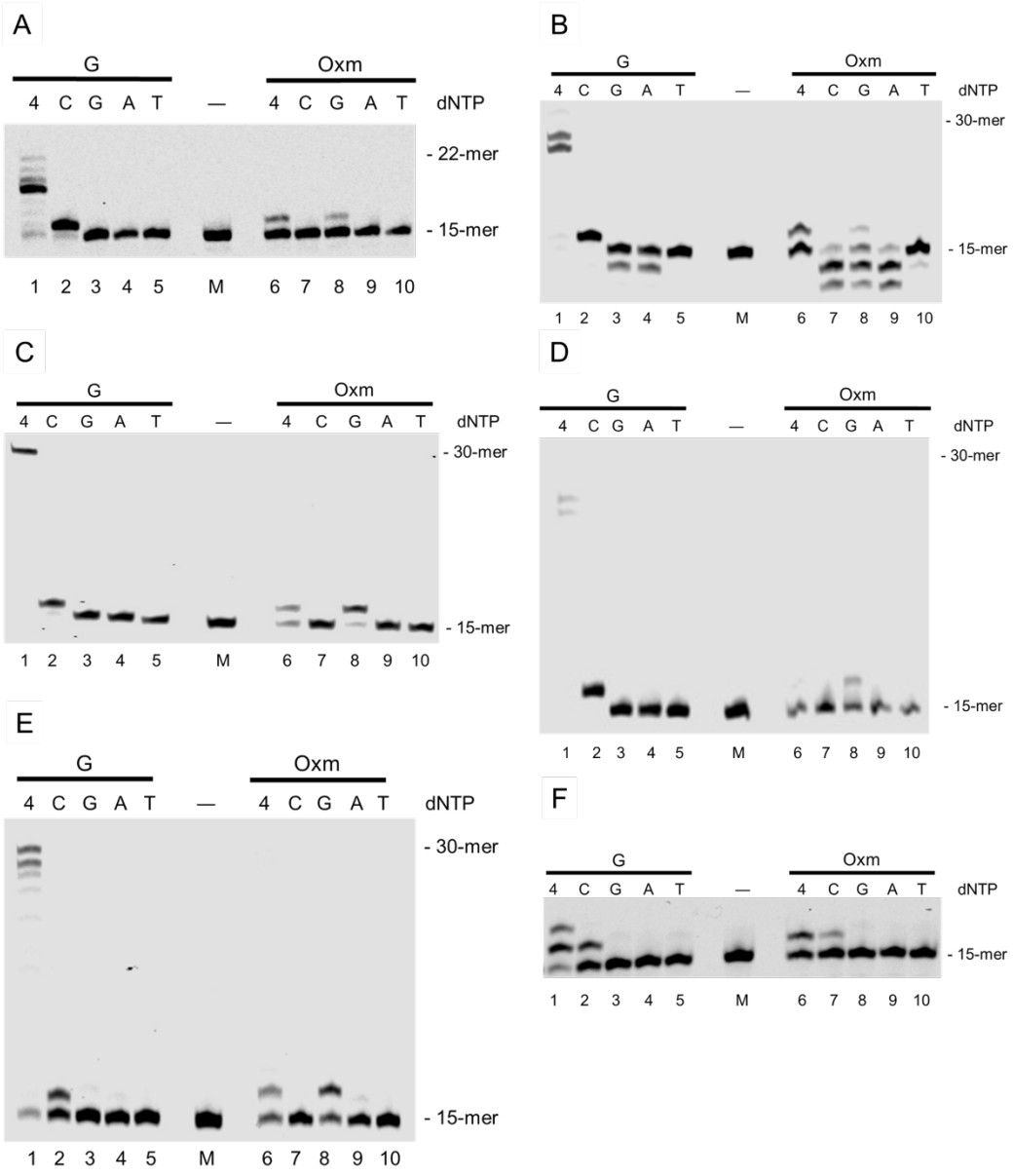

Figure S7. DNA synthesis and selective nucleotide incorporation opposite Oxm by DNA polymerase β, *Pyrobest* DNA polymerase (Pyrobest), Taq DNA polymerase (Taq), Vent DNA polymerase exo$^-$ (Vent exo$^-$), Klenow fragment exo$^-$ (Kf exo$^-$), and hREV1$_{(341\text{-}829)}$. DNA polymerase β (250 μU) (A), Pyrobest (125 μU) (B), *Taq* (75 mU) (C), *Vent* exo$^-$ (167 nU) (D), Kf exo$^-$ (75 μU) (E), and hREV1$_{(341\text{-}829)}$ (1.7 ng) (F) were incubated with templates containing G (lanes 1–5) or Oxm (lanes 6–10) and 100 μM of either all four dNTPs (lanes 1 and 6) or 100 μM of a single dNTP (N = C, G, A, or T) (lanes 2–5 and 7–10). Lane M contained no enzyme and served as a negative control.

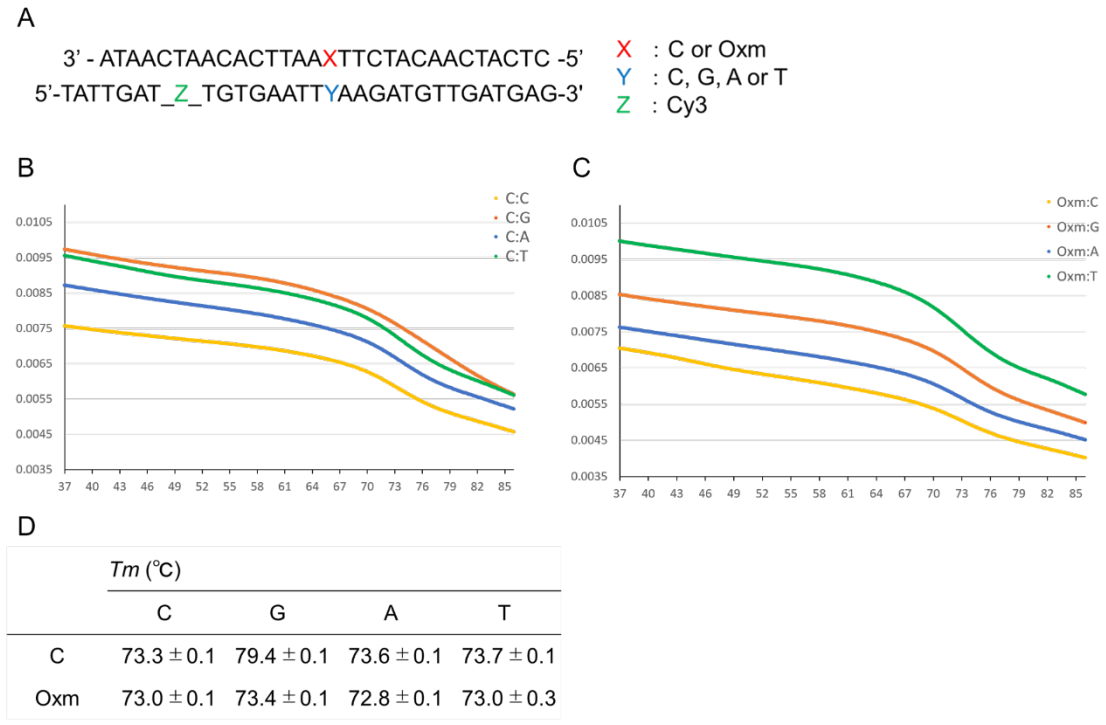

Figure S8. Analysis of melting temperature (*Tm*). (A) DNA sequences used in this experiment. (B) Analysis of *Tm* for cytosine as a control. (C) Analysis of *Tm* for Oxm. (D) Comparison of *Tm* values for cytosine and Oxm.

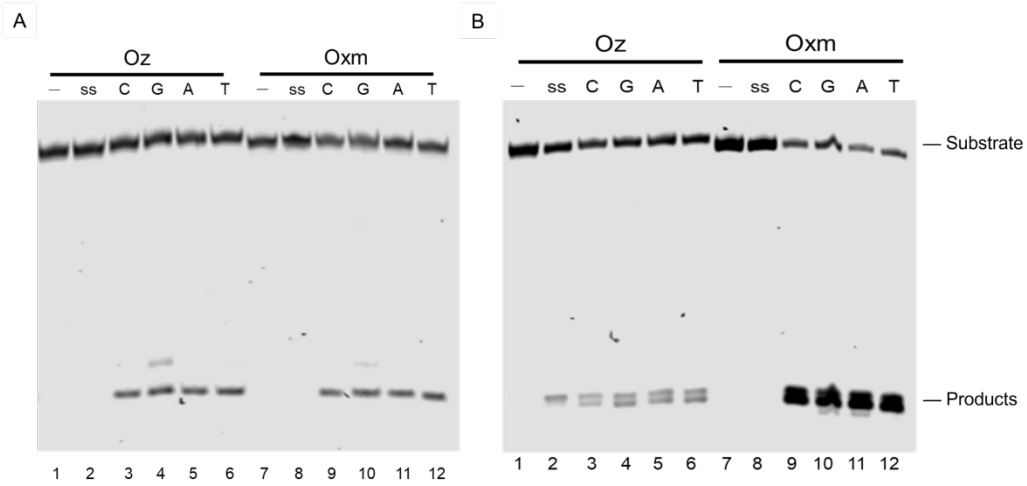

Figure S9. Incision activities of Nei and Nth. (A) Nei (71 mU) incubated with templates containing C, G, A, or T (lanes 3–6 and 9–12) and Alexa 680-labeled DNA oligomers containing Oz (lanes 1–6) or Oxm (lanes 7–12). (B) Nth (500 mU) incubated with templates containing C, G, A, or T (lanes 3–6 and 9–12) and Alexa 680-labeled DNA oligomers containing Oz (lanes 1–6) or Oxm (lanes 7–12).

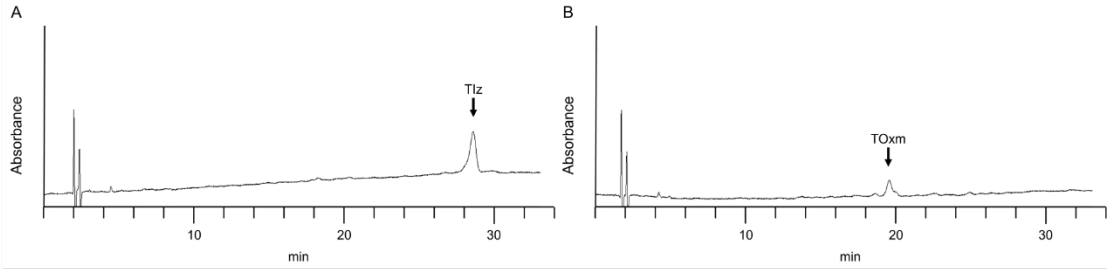

Figure S10. Quick generation of TOxm. (A) HPLC analysis of the reaction mixture containing Iz. (B) HPLC analysis of the solution in (A) after pyrolysis for 10 min. The reaction mixture was prepared to maximize the amount of TIz from TG using LED irradiation (450 nm). This reaction mixture was used as the starting material to rapidly generate TOxm from TIz. The mixture containing Iz was incubated at 90°C for 10 min under basic conditions (pH 13). TOxm was generated from TIz with 29% efficiency. Samples were analyzed by HPLC using a COSMOSIL PBr packed column (Nacalai Tesque; 5 μm, 150 × 4.6 mm) with a solvent gradient of 50 mM TEAA (pH 7) and 3–6% CH_3CN over 20–35 min at a flow rate of 1.0 mL/min. Absorbance was monitored at 254 nm.

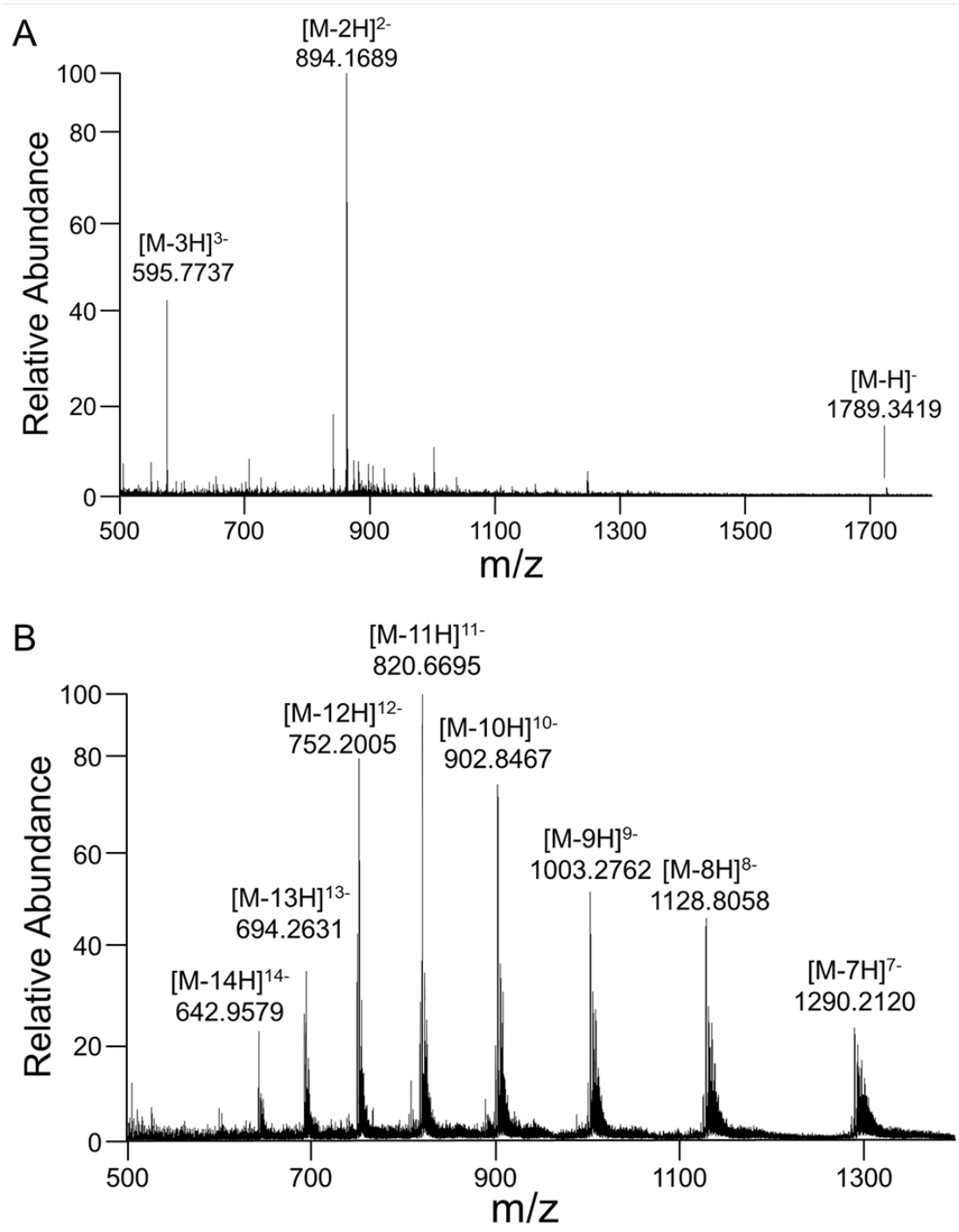

Figure S11. Mass spectra of (A) 6-mer Oxm and (B) 30-mer Oxm.